



AD-A272 233



## **INTERLEAVED BISMALIMIDE COMPOSITES**

Eileen Armstrong-Carroll and Thomas M. Donnellan  
Air Vehicle and Crew Systems Technology Department (Code 6064)  
NAVAL AIR WARFARE CENTER  
AIRCRAFT DIVISION WARMINSTER  
P.O. BOX 5152  
Warminster, PA 18974-0591

**1 DECEMBER 1992**

**FINAL REPORT**  
Period Covering July 1989 to May 1991  
P.E. 62234N  
P.N. RS-34ASO

*Approved for Public Release; Distribution is Unlimited.*

**93-27313**



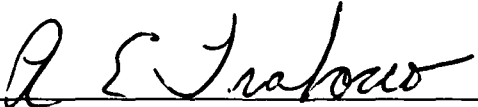
Prepared for  
Air Vehicle and Crew Systems Technology Department (Code 6064)  
NAVAL AIR WARFARE CENTER  
AIRCRAFT DIVISION WARMINSTER  
P.O. BOX 5152  
WARMINSTER, PA 18974-0591


## NOTICES

**REPORT NUMBERING SYSTEM** — The numbering of technical project reports issued by the Naval Air Warfare Center, Aircraft Division, Warminster is arranged for specific identification purposes. Each number consists of the Center acronym, the calendar year in which the number was assigned, the sequence number of the report within the specific calendar year, and the official 2-digit correspondence code of the Functional Department responsible for the report. For example: Report No. NAWCADWAR-92001-60 indicates the first Center report for the year 1992 and prepared by the Air Vehicle and Crew Systems Technology Department. The numerical codes are as follows:

CODE	OFFICE OR DEPARTMENT
00	Commanding Officer, NAWCADWAR
01	Technical Director, NAWCADWAR
05	Computer Department
10	AntiSubmarine Warfare Systems Department
20	Tactical Air Systems Department
30	Warfare Systems Analysis Department
50	Mission Avionics Technology Department
60	Air Vehicle & Crew Systems Technology Department
70	Systems & Software Technology Department
80	Engineering Support Group
90	Test & Evaluation Group

**PRODUCT ENDORSEMENT** — The discussion or instructions concerning commercial products herein do not constitute an endorsement by the Government nor do they convey or imply the license or right to use such products.

Reviewed By:  Date: 8/2/93  
Branch Head

Reviewed By:  Date: 8-2-93  
Division Head

Reviewed By:  Date: 8-25-93  
Director/Deputy Director

**REPORT DOCUMENTATION PAGE**Form Approved  
OMB No. 0704-0188

Public reporting burden for this collection of information is estimated to average 1 hour per response, including the time for reviewing instructions, searching existing data sources, gathering and maintaining the data needed, and completing and reviewing the collection of information. Send comments regarding this burden estimate or any other aspect of this collection of information, including suggestions for reducing this burden, to Washington Headquarters Services, Directorate for Information Operations and Reports, 1215 Jefferson Davis Highway, Suite 1204, Arlington, VA 22202-4302, and to the Office of Management and Budget, Paperwork Reduction Project (0704-0188), Washington, DC 20503.

1. AGENCY USE ONLY (Leave blank)		2. REPORT DATE 1992	3. REPORT TYPE AND DATES COVERED FINAL (JULY 89 - MAY 91)	
4. TITLE AND SUBTITLE  INTERLEAVED BISMALEIMIDE COMPOSITES			5. FUNDING NUMBERS  PROGRAM ELEMENT NO. 62234N  PROJECT NO. RS-34AS0	
6. AUTHOR(S)  EILEEN ARMSTRONG-CARROLL and THOMAS M. DONNELLAN				
7. PERFORMING ORGANIZATION NAME(S) AND ADDRESS(ES)  NAVAL AIR WARFARE CENTER AIRCRAFT DIVISION WARMINSTER (CODE 6064) P.O. BOX 5152 WARMINSTER, PA 18974-0591			8. PERFORMING ORGANIZATION REPORT NUMBER  NAWCADWAR-92102-60	
9. SPONSORING / MONITORING AGENCY NAME(S) AND ADDRESS(ES)  NAVAL AIR WARFARE CENTER AIRCRAFT DIVISION WARMINSTER (CODE 6064) P.O. BOX 5152 WARMINSTER, PA 18974-0591			10. SPONSORING / MONITORING AGENCY REPORT NUMBER  NAWCADWAR-92102-60	
11. SUPPLEMENTARY NOTES				
12a. DISTRIBUTION / AVAILABILITY STATEMENT  APPROVED FOR PUBLIC RELEASE; DISTRIBUTION IS UNLIMITED.			12b. DISTRIBUTION CODE	
13. ABSTRACT (Maximum 200 words)  <p>This report examines interleaving as a technique for the improvement of delamination resistance in composites. In particular, the influence of the deformation behavior of the interleaf film and film adhesion on composite fracture energy is studied. Teflon, E, and Kapton interleaf film materials are compared. Kapton and E films display predominantly brittle deformation behavior. Teflon exhibits substantial deformation before failure. All films are plasma treated to vary film-resin bond strengths. With the Kapton and Teflon films, plasma treatments are shown to increase film-resin adhesion and fracture energy. The effectiveness of Teflon as an interleaf material may be limited by the toughness of this film. Film-resin adhesion with the E film is determined to be optimized. Fracture energy is greatest with composites interleaved with the E film.</p>				
14. SUBJECT TERMS  POLYMER MATRIX COMPOSITES, INTERLEAVED COMPOSITES, PLASMA TREATMENT, BISMALEIMIDE.			15. NUMBER OF PAGES	
			16. PRICE CODE	
17. SECURITY CLASSIFICATION OF REPORT UNCLASSIFIED	18. SECURITY CLASSIFICATION OF THIS PAGE UNCLASSIFIED	19. SECURITY CLASSIFICATION OF ABSTRACT UNCLASSIFIED	20. LIMITATION OF ABSTRACT UL	

# CONTENTS

	PAGE
FIGURES .....	iv
TABLES .....	vi
ACKNOWLEDGEMENTS.....	vii
INTRODUCTION .....	1
MATERIALS .....	3
PROCEDURES .....	3
PLASMA TREATMENTS .....	3
CONTACT SURFACE ANGLE MEASUREMENTS .....	4
FOURIER TRANSFORM INFRARED SPECTROSCOPY (FTIR) .....	4
MICROSCOPY .....	5
PROCESSING PROCEDURES .....	5
MECHANICAL TESTS .....	5
RESULTS AND DISCUSSION.....	7
INTERLEAF FILM CHARACTERIZATION.....	7
INTERLEAVED COMPOSITE CHARACTERIZATION .....	10
CONCLUSIONS .....	13
REFERENCES .....	15

DTIC QUALITY INSPECTED 8

Accession For	
NTIS	CRA&I
DTIC	TAB
Unannounced	
Justification	
By	
Distribution	
Avail	
Dist	
A-1	

# FIGURES

Figure		Page
1.	Illustration Of The Interleaving Concept. ....	17
2.	Possible Interleaf Film-Resin Bonding Mechanisms. Schematic Depicts How Grafted-Allylamine Polymer Acts As A Coupling Agent Between The Interleaf Film And BMI Resin. ....	18
3.	Schematic Of The Process Through Which Process Gases Are Excited And Deposited On The Interleaf Films. ....	19
4.	Possible Surface Chemistries Produced With Argon, Ammonia, And Allylamine Plasma Treatments. The Filled Circles Represent Carbonyl Free Radicals Formed During Plasma Treatment. ....	20
5.	Illustration Of How Contact Angle Is Measured And Critical Surface Tension Is Determined. ....	22
6.	Processing Cycle For Interleaved Cycom 3100/IM6. ....	23
7.	Schematic Of The Flatwise Tension Test Set-Up. ....	24
8.	Depiction Of The Typical Test Sequence For The Resin-Drop Shear Test. ....	25
9.	Schematic Of The Floating Roller Peel Test Set-up. ....	26
10.	Transmission Spectra Of Untreated And Plasma Treatment One Teflon. Three Allylamine Valleys Are Visible On Spectra Of Plasma Treated Teflon Collected From A Salt Tablet And An ATR Crystal At $3000\text{cm}^{-1}$ , $2100\text{cm}^{-1}$ , And $1600\text{cm}^{-1}$ . ....	27
11.	Reproducibility Of Plasma Treatments As Collected With Salt Tablets Placed In The Plasma Reactor During Film Treatment. Seven Different Batches Of Teflon Treatment One Are Plotted. ....	28
12.	Reproducibility Of Plasma Treatments as Collected With ATR Spectra Of Treated Films. Five Different Regions Of A Teflon Treatment One Film Are Plotted. ....	29
13.	Absorption Spectra Of Plasma Treated Teflon. The Differences In Peak Intensity Due To The More Severe Plasma Treatment Are Greater Than Those Due To Variations In Reproducibility. ....	30
14.	Untreated Teflon Film. Topography Is Marked By A Dendritic Structure. ....	31
15.	Teflon Film Treated With Treatment Two. Valleys In Film Topography Are Partially Obscured By Grafted Allylamine. ....	32
16.	Teflon Film Treated With Treatment Three. Original Teflon Topography Is Totally Obscured By Plasma Treatment. ....	32

FIGURES (Continued)

Figure		Page
17.	Kapton Film Treated With Treatment Two. Similar To Untreated Kapton Film Topography. ....	33
18.	Untreated Kapton Film Failed In Tension. Failure Surface Is Featureless.....	33
19.	Kapton Film Treatment Two Failed in Tension. Failure Surface Possesses Several Vertical Cleavage Striae.....	35
20.	Untreated Teflon Film Failed In Tension. Outer Film Layers Deform And Tear Away From Film. Material Behaves In This Manner Since It Is Composed Of Several Thin Cast-Teflon Layers.....	35
21.	Teflon Film Treatment Three Failed In Tension. Failure Surface Marked By Several Vertical Cleavage Striae. Within Each Stria The Failure Surface Is Cleaved At Several Locations.....	36
22.	Spectrum Of An ENF Failure Surface Compared With Spectrum Of A Plasma Treated Film For Kapton Treatment Two. Allylamine Valleys Are Absent On The ENF Failed Film Surface.....	39
23.	Spectrum Of ENF Failure Surface Compared With Spectrum Of Plasma Treated Film For Teflon Treatment Three. Allylamine Valleys Are Absent On The ENF Failed Film Surface.....	40
24.	Cycom 3100/IM6 Composite Failed Through ENF Testing. Fracture Energy Absorbed Through Resin Fracture. ....	41
25.	Cycom 3100/IM6 Composite, Interleaved With Kapton Failed Through ENF Testing. Additional Fracture Energy Absorbed Through Film Tearing. ....	41
26.	Cycom 3100/IM6 Composite, Interleaved With Kapton Treatment Two, Failed Through ENF Testing. More Deformation Is Evident At Film Tearing Sites. Some Hackles Are Evident.....	42
27.	Cycom 3100/IM6 Composite, Interleaved With E-Film, Failed Through ENF Testing. Film Tears And Deforms. Hackle Possesses Ductile Features. ....	43
28.	Cycom 3100/IM6 Composite, Interleaved With Teflon Treatment Two, Failed Through ENF Testing. Plastic Deformation Is Subtle.....	43
29.	Cycom 3100/IM6 Composite, Interleaved With Teflon Treatment Two, Failed Through ENF Testing. Cratered Surface Denotes Extensive Local Deformation Of Teflon Film. ....	44
30.	Cycom 3100/IM6 Composite, Interleaved With Teflon Treatment Three, Failed Through ENF Testing. Extensive Tearing And Stretching Of Teflon Film.....	44

TABLES

Table	Page
1. Interleaf Film Plasma Treatments .....	21
2. Tensile Properties Of Interleaf Films .....	34
3. Peel Test Results .....	37
4. ENF Test Results .....	38

**ACKNOWLEDGEMENTS**

The authors would like to thank D. Alley, B. Duffy, S. Kwong, J. Katilaus, B. Pregger, and K. Hutchins for their assistance in specimen preparation and testing. The authors would also like to thank I. Kamel and B. Iskandarani of Drexel University for the assistance in developing plasma treatments and for performing plasma treatments on the interleaf films. The authors would like to thank Dr. Frank Ko of Drexel University for the use of the Kawabata testing machine.



## INTRODUCTION

The goal of this program was to characterize interleaving as a method to improve damage tolerance in BMI composites. The increased thermal and structural requirements of emerging aircraft designs necessitate the use of composites which operate in the 350-400°F temperature range. Bismaleimide (BMI) composites possess the required strength and heat stability properties. Thus these materials have received a great deal of attention for composite structures. First generation BMI resins are extremely brittle and display microcracking after processing or repeated thermal exposure. The brittle nature of BMIs render them more sensitive to impact and delamination than epoxy materials.

In composites there is a correlation between resin brittleness and damage tolerance as measured by compressive strength after impact (CAI) [1]. Brittle BMI composites have CAI values of approximately 124-138 MPa (18-28 ksi) [8] based on the Boeing version of the test. Conventional epoxy based composites by comparison have CAI strengths in the range of 172-276 MPa (25-40 ksi) [7]. The damage sensitivity of these materials affects both design efficiency and materials selection for composite components in aircraft.

Currently a number of approaches are being investigated for the improvement of the damage tolerance of brittle matrix composites. These approaches are resin formulation modification, through-thickness fibrous reinforcement, and interleaving. Formulation approaches center on the addition of ductile rubber or thermoplastic constituents to the resin which act to increase the fracture energy of the resin [2]. One variant of this approach is the formulation of multiple phase resins which separate spatially in the composite during processing [3]. Physical reinforcement approaches, such as stitching and braiding, improve impact resistance via out-of-plane fiber orientations [4]. These fiber orientations allow for more effective stress translation through the fibrous reinforcements after an impact event. With resin formulation and physical reinforcement techniques, some compromise in thermal stability or in-plane structural properties is accepted in order to improve the damage tolerance of the composite. The interleaving approach for improvement of damage tolerance involves the insertion of films of adhesive or thermoplastic materials at the interply interfaces in composite laminates. A schematic of an interleaved composite is depicted in Figure 1.

Some research has been conducted on epoxy and BMI interleaved composites [5-12]. Epoxy composites have been evaluated with tough epoxy adhesives as interleaves [5,7,10,11,12]. Research conducted on epoxy interleaved composites has shown that the material used as the interleaf must have high strain to failure for energy absorption during fracture and must possess a high modulus for retention of composite properties [9]. Also tailoring of the film thickness and film-resin interdiffusion provides a good combination of toughness and in-plane properties [6].

Interleaved BMI composites have also been investigated [5,7,9-12]. With this matrix material thin thermoplastic films appear to be the most effective interleaf materials. One film in particular, the "E" film, provides CAI values of 214 MPa (31 ksi) in an Cycom 3100/IM6 composite system [12]. This is a 50% improvement from baseline properties. Increases in CAI can be predicted from the fracture energy in shear,  $G_{IIC}$  [12]. Results from previous work indicate that the degree of improvement in interleaved composites is limited by the amount of adhesion between the film and the BMI resin [7,12]. This conclusion is based on a comparison of the surface deformation characteristics observed on the interleaf and resin in epoxy and BMI composite samples.

One technique to evaluate the effects of film adhesion is through radio frequency (RF) plasma treatment. Plasma treatments are commonly used for surface modification of films and fibers [12-15]. Plasma technology provides a valuable means of modifying surface structure and the composition of materials without altering bulk properties. Plasma treatments typically produce altered regions which range from angstroms to microns in thickness. In the present research the influence of film adhesion is investigated using plasma treatments to modify the film surface and to add sites for chemical bonding between the film and resin. A mechanism through which a plasma deposited layer adds sites for chemical bonding between the film and resin is depicted in Figure 2. With this mechanism a chemical reaction between the amine groups (provided by the grafted layer) and bismaleimide resin is expected to occur at the interface during the curing cycle. Thus the plasma-deposited layer can increase the film-resin bond by acting as a coupling agent.

The goal of this study was to maximize the film-resin bond through the use of plasma treatments. As a result of film characterization, plasma evaluation and interleaved composite testing, several testing techniques to quantify film-resin adhe-

sion and fracture toughness of interleaved composites were evaluated in this program. This report summarizes a research program which examined several important aspects of damage tolerance improvements using interleaves. The aspects of interleaving studied include plasma chemistry, deposition conditions and mechanical properties of interleaf films.

## **MATERIALS**

The films studied are 12.7 microns thick. The film materials are a kapton polyimide film from Dupont, a "E" film from American Cyanamid, and a teflon film from ChemFab. The films are incorporated into composites with American Cyanamid Cycom IM6/3100 BMI prepreg material.

## **PROCEDURES**

### **PLASMA TREATMENTS**

All films are solvent cleaned with toluene or acetone prior to treatment. Plasma treatments are performed in a Branson IPC 3000 series 13.5 MHZ Rf plasma reactor. The plasma deposition procedure used is diagrammed in Figure 3. In this procedure the plasma reactor excites the incoming gases. The resultant plasma contains several energetic, highly-reactive species. These species etch, break bonds and generate free radicals on the film surface. Some of these species emit photons. The photons generate UV light. The UV light induces plasma polymerization and crosslinking reactions.

For this program films are plasma treated in a two step process which involves an argon etch followed by an ammonia plasma deposition or an allylamine polymerization. A possible reaction mechanism between interleaf films and the different plasmas is shown in Figure 4. In this case the argon plasma generates a carbonyl radical on the film surface. The argon etch also removes surface impurities. The subsequent ammonia or allylamine plasma treatments could form an amide linkage with this radical. The resultant amine groups react with the BMI resin. When the ammonia plasma is used, the amine groups are randomly dispersed. The molecular structure of the allylamine polymer results in a more uniform distribution of amine groups. For this plasma treatment the allylamine monomer is polymerized in the plasma atmosphere and then condensed on the interleaf film in the plasma chamber.

The process variables are plasma power, pressure, and time. The experimental conditions control the chemistry and thickness of the coating. Higher plasma power levels increase the concentration of excited species and with allylamine, increase crosslink density. Higher pressure levels increase the allylamine condensation rate. The plasma polymerized layer thickness increases with plasma exposure time. Initial treatment levels were selected based on earlier work [13]. The plasma treatments examined are summarized in Table 1.

#### CONTACT SURFACE ANGLE MEASUREMENTS

Measurements are performed with a Rame Hart NRL C-A Goniometer (Model 100-00-115). A series of water/methanol solutions with known surface tensions are used. Surface angle measurements are made at 77°F. Critical surface tensions for the films studies are determined with the technique depicted in Figure 5 [16].

#### FOURIER TRANSFORM INFRARED SPECTROSCOPY (FTIR)

Fourier transform infrared spectroscopy is performed with a Perkin Elmer 1800 FTIR with a  $4\text{ cm}^{-1}$  accuracy. With FTIR, resonance of chemical bonds at infrared frequencies cause infrared radiation to be absorbed. Film coating thickness and chemistry are monitored with sodium chloride salt tablets exposed with the films in the plasma chamber. Isolation of peaks due to the extremely thin coatings from the bulk film material is not possible with conventional FTIR spectroscopy. FTIR spectroscopy with an Attenuated Total Reflection (ATR) sample mount is performed on plasma treated films and End Notch Flexure (ENF) failure surfaces. With ATR infrared radiation propagates through the germanium crystal and enters the specimen at an angle close to the critical angle. The depth of penetration into the specimen ranges from less than a micron to a few microns as a function of wavelength. ATR spectra were obtained with a trapezoidal germanium crystal possessing an incident angle of 60 degrees. Spectra are plotted in transmission as a function of wavelength. No units are given for the vertical axes when the FTIR plots are staggered for comparison. When the plots are staggered, the shape of the plots can be compared but the relative magnitude of valleys cannot be compared. Relative thickness measurements are made from the relative peak intensities of absorption spectra. The carbon dioxide peak at  $2360\text{ cm}^{-1}$  is an experimental artifact.

## MICROSCOPY

Surfaces of fractured specimens are gold sputtered. The plated surfaces are examined with optical and scanning electron microscopy (SEM). A Nikon optical microscope is used for the optical microscopy. An Amray model AMR 1000 microscope is used for the SEM work.

## PROCESSING PROCEDURES

All composite panels (including panels with no interleaf film) are processed with the recommended cure and post-cure procedures for interleaved Cycom 3100/IM6 developed by American Cyanamid. The processing cycle is diagrammed in Figure 6.

## MECHANICAL TESTS

*Film Tensile Test:* Tensile tests are performed according to ASTM standard D882-81, Tensile Properties of Thin Plastic Sheeting. The tests are performed with a model 1122 table top Instron machine. The gage length used is 5.08 cm. A cross-head speed of 2.54 cm/min is used for the kapton film. A cross-head speed of 50.8 cm/min is used for the teflon film.

*Composite Flatwise Tension Test:* The flatwise tension test performed is a modification of ASTM C297, Tension Test of Flat Sandwich Constructions in Flatwise Plane. Each sample is a 5.1 by 5.1 cm square with the following lay-up geometry,  $[0/+45/0/-45/0]_s$ , interleaf film,  $[0/+45/0/-45/0]_s$ . Specimens are adhered to aluminum blocks with FM300K adhesive. A schematic of the partially assembled flatwise tension fixture and specimen is shown in Figure 7. Cross-head speeds used are either 0.013, 0.05, or 0.13 cm/min. This rate is adjusted so that the maximum load will occur between 3 and 6 minutes of test time. Flatwise tension tests are performed with a model TT-D Instron machine.

*Double Cantilever Beam Test (DCB):* The double cantilever beam test is performed using the July 1983 NASA version of ST-5: Specification of Hinged Double Cantilever Beam Test. The values for mode one fracture toughness recorded in this paper are calculated using the modified direct beam method. DCB tests are performed with a model 1122 table top Instron machine.

## NAWCADWAR-92102-60

**Resin-Drop Shear Test:** Resin droplets are cured onto an interleaf film. Circular holes 2.4mm in diameter are punched from a 0.8mm thick piece of silicon rubber. The rubber is placed on top of an interleaf film. Resin is heated to minimum viscosity and inserted into the circular holes. The assembly is cured for 5 hours at 177°C. A piece of film is folded so a resin-drop is located in the same position on either side. The sample is loaded onto a Kawabata testing machine with a fiber-pullout grip set-up. Knife-edge jaws force the resin to shear off the film. A schematic of the testing sequence is depicted in Figure 8. For this test a 5kg load cell is used. The cross-head speed is 0.005cm/sec.

**Lap Shear Test:** Two 2.5 cm by 10.1cm ply-packs are stacked with an 1.3 cm overlap. Two different ply pack lay-ups are used. The first is one 0° ply. The second is a 0°/90°/0° lay-up. An interleaf film is placed in the overlap region. Release films are used to fill the area under the upper ply pack and over the lower ply pack. The release film also prevents excess resin from bridging in the overlap region. The assembly is cured for 4 hours at 177°C in an hydraulic press. The cured assembly is loaded in tension with a model 1122 table top Instron machine. A cross-head speed of 12.5 cm/min is used.

**Composite Peel Test:** The peel test performed is a modification of ASTM D3167 - 76, Floating Roller Peel Resistance of Adhesives. Samples are 2.54 by 17.4 cm long. The laminate geometry used is  $[0/+45/0/-45/0]_s$ . A disbond area of 7.6 cm is created with a 12.7 micron teflon or freekoted kapton film. The disbond area is used to thread the specimen through the floating rollers. A schematic of the test set-up is shown in Figure 9. The interleaf films are backed with a 0° ply of Cycom 3100 to inhibit plastic deformation and tearing. The cross-head speed is 12.7 cm/min. Peel tests are performed with a model 1122 table top Instron machine. The peel load is measured in 0.25 cm increments.

**End Notch Flexure Test (ENF):** The end notch flexure test performed is based on ASTM D30.02 ENF test round robin instructions. ENF tests are performed on a model 1122 table top Instron machine. Crack starter film inserts are 3.2 cm long and are composed of 12.7 micron teflon. Precracks approximately 4 cm long are created using a razor blade. Coupons are placed in the three point bend loading fixture so that the end of the precrack region is located halfway between the upper and lower

loading nose. A crosshead speed of 2.54 mm/min is used. The beam theory calculation method for determining mode two critical crack propagation energy is used. The compliance value is measured directly from the load deflection curve for each sample.

## RESULTS AND DISCUSSION

### INTERLEAF FILM CHARACTERIZATION

*Chemistry and Reproducibility of Plasma Treatments:* The surface chemistry of the plasma treated films is characterized with FTIR spectroscopy using an ATR crystal. The chemistry of the plasma polymerized allylamine is also documented with FTIR spectroscopy on salt tablets. A previous work [15] assigns the following functional groups to plasma polymerized allylamine:  $3000 - 2800 \text{ cm}^{-1}$  - aliphatic carbon single bond hydrogen stretching,  $2190 \text{ cm}^{-1}$  carbon triple bond nitrogen stretching, and  $1630 \text{ cm}^{-1}$  carbon double bond nitrogen stretching. Figure 10 shows spectra of untreated teflon and teflon treatment number one. Both salt tablet and ATR crystal FTIR spectrum collection techniques are shown in this figure. The spectra of the treated samples exhibit the three allylamine signature valleys. Thus both ATR and salt tablet collection techniques characterize plasma treatment chemistry. Note the absence of these peaks with the untreated film spectrum. Similar results are observed with treated versus untreated kapton FTIR spectra.

FTIR spectra also provide information on the reproducibility of the plasma treatments. Figure 11 shows the reproducibility of the teflon number one plasma treatment process for seven different plasma runs. In general the treatments are chemically reproducible. Although some variability in spectra occurs, most of this variability can be attributed to baseline differences in the salt tablets.

Reproducibility within five areas from the same teflon film is depicted in Figure 12. Variability in coating thickness is more apparent in this figure. This variability is due to heterogeneity in plasma flow field over the large surface area of the film being treated.

FTIR spectra show that the differences between spectra due to different plasma treatments is significantly greater than the scatter within a given treatment. Figure 13 depicts spectra obtained with teflon plasma treatments one and three. The differences in treatment one and treatment three spectra are significantly greater than

those between the two treatment one spectra shown. These differences are quantified by measuring the intensity of the  $1630\text{ cm}^{-1}$  absorbance peak. There is a thirty percent scatter in peak intensity within the batch runs of teflon treatment one. The  $1630\text{ cm}^{-1}$  peak intensity of the teflon treatment three spectrum is one hundred sixty percent greater than the most intense teflon treatment one peak. The increases in peak intensity correspond with increases in the number of allylamine functional groups. The peak intensities are indicative of the relative thickness of the grafted allylamine layer. The ratio between the carbon triple bond nitrogen and the carbon double bond nitrogen peak increases with plasma treatment severity. This increase denotes changes in the chemistry of the allylamine layer. The increases of plasma treatment power, time, and pressure in treatment three are responsible for these differences.

FTIR spectra of untreated and treated kapton show results similar to the teflon results documented in this section.

Another technique used to examine plasma treatment reproducibility is contact angle measurements. Plasma treatments increase the wetting behavior of the interleaf films. Since the wetting behavior of kapton and the E films is already fair, variations in methanol concentration did not effect the contact angle greatly. Thus contact angle measurements are not sensitive enough to detect differences between surface treatments. However contact angle measurements can distinguish between treated and untreated films.

*Film Surface Topography:* SEM microscopy shows evidence of surface topographical changes induced by the plasma treatments. Figures 14 to 16 show the surfaces of teflon in an untreated state and after two different treatments. An effect of the treatments is to increase the coating thickness of the allylamine which eventually covers teflon surface characteristics.

The treated kapton film surface is smooth and featureless (Figure 17). The topography of untreated kapton is also smooth and featureless. Thus SEM techniques cannot distinguish smoothing due to grafted allylamine on the surface of kapton films.

*Tensile Properties of Interleaf Films:* The results of the tensile tests performed on the film materials are shown in Table 2. An examination of the untreated film



properties shows that there is a significant difference in the deformation behavior of the interleaf films. The E-film has the highest yield strength. The yield strength of the kapton is approximately one-half that of the E-film. The teflon film possesses the lowest yield strength, approximately one-tenth that of the E-film. The kapton film possesses the highest modulus. The modulus of the E-film is approximately two-thirds that of the kapton. Teflon has the lowest modulus which is approximately two orders of magnitude lower than the kapton. The failure strength of the E-films is approximately 75% that of kapton. The failure strength of teflon is approximately 15% that of kapton. The kapton and E films both fail in a brittle manner with very little plastic deformation. The teflon film deforms extensively prior to failure.

The modulus of the teflon films increases with plasma treatment. The effect of plasma treatment on the kapton and teflon film properties is to reduce the film tensile strength and elongation. There are a number of possible explanations for these reductions. The reductions could be the result of surface embrittlement due to chain scission, a film surface roughening effect, or modification of the mechanical properties of the film's surface due to the plasma coating.

A comparison of the surfaces of tested tensile specimens from the treated and untreated films (Figures 18 to 21) indicates that the grafted-allylamine layer embrittles the film surface. The allylamine layer fails by cleavage. The vertical striations in Figures 19 and 21 indicate a brittle failure mode. The amount of deformation at failure is greater in the teflon film, and the surface striations are more widely spaced. The increased ability of teflon to plastically deform and tear as well as the high strain rate used in testing the teflon films contribute to the effect observed.

The results indicate that the coating deposited by the argon/allylamine treatment embrittles the film surface and lowers the failure strain of the treated films. It would be expected that the effectiveness of these film materials as interleafs is adversely affected by the embrittlement of the surface. The diminished failure strain and strength of the treated materials may indicate that the notch sensitivity of the film materials is increased with the argon/allylamine plasma treatment. Clearly plasma treatments can significantly alter the material properties of interleaf films.

## INTERLEAVED COMPOSITE CHARACTERIZATION

*Film-Resin Adhesion:* Flatwise tension, resin-drop shear, lap shear, and peel tests are used to characterize film-resin adhesion. All of these test methods are limited in ability to characterize film-resin adhesion.

Flatwise tension specimens fail at the film-resin interface when film-resin adhesive strength is less than interlaminar strength of the composite plies. This is the case with the kapton and teflon interleaf films. With the E-film, interleaf film-resin adhesive strength is greater than interlaminar strength. E-film interleaved composites did not fail in the plane of the film. E-film interleaved composite failure occurs in the composite layers through a thickness of several plies. Scatter in failure stress with kapton interleaved specimens is high. The high amount of scatter may be attributed to the variability with which the interleaf films tears at the film-resin interface. The significant level of scatter precludes the use of this test other than as a test of the strength being greater or less than the interlaminar strength of the composite.

Although the resin-drop shear test can measure film-resin adhesion for all interleaf films tested, the large amount of scatter associated with this test diminishes its significance. This scatter is due to the lack of symmetry between the two droplets which are sheared simultaneously.

The lap shear test can only measure film-resin adhesion when the film-resin bond is relatively weak. When film-resin adhesion is higher out-of-plane loading begins to occur within the ply packs.

Results from peel tests are listed in Table 3. The peel strength of the E-film is much higher than that of the other interleaf films. Plasma treatments reduce film-resin adhesion with the E-film. This reduction is not significant when peel strength variability is considered (With E-film one standard deviation is equal of  $0.3\pi w$ ). Film-resin adhesion is relatively unaffected by plasma treatment with the kapton film. Plasma treatments gradually increase film-resin adhesion with the teflon film. Due to the low peel strength values, the noise level associated with slight variations in the peel angle and a slip-stick phenomena produces large variations in peel strength within a sample. This variation renders the peel test inadequate as an indicator of film-resin adhesive strength.

*Fracture Toughness:* Both modes one (tensile) and mode two (shear) fracture toughness test are performed on control and interleaved composites. The Double Cantilever Beam (DCB) test propagates a crack in tension. The Edge Notch Flexure (ENF) test propagates a crack in shear.

The usefulness of DCB testing is limited when film-resin adhesion is low or high. When film-resin adhesion is low, as with the kapton and teflon films, the crack propagates too quickly and propagates significantly when the specimen is unloaded. Thus the specimen quickly reaches the large deflection region and actual crack length cannot be measured. When film-resin adhesion is high, as with the E-film, the crack quickly propagates out-of-plane. The use of this test method is precluded by these factors.

ENF testing is a suitable test method for all interleaved composites tested. The scatter associated with this test method is low enough for different plasma treatments to significantly alter ENF test results. End Notch Flexure test results are shown in Table 4. The untreated kapton film possesses a  $G_{IIC}$  similar to that of the uninterleaved material. The similar  $G_{IIC}$  values indicate that the energy absorbed in film deformation and fracture must be equivalent to that absorbed during resin fracture in the uninterleaved material. Plasma treatment of the kapton provides an approximately 100 percent improvement in  $G_{IIC}$ . With the ammonia plasma treatments  $G_{IIC}$  increases with treatment severity. Treatment two is more severe than one due to the additional time allotted for ammonia deposition. The increases in power, pressure, and time with ammonia treatment three increase polymerization rate, deposition rate, and the quantity deposited respectively. The most severe kapton allylamine film treatment (treatment number 2) possesses a slightly lower  $G_{IIC}$  value than kapton allylamine treatment one. The  $G_{IIC}$  values of kapton treatments one and two are within a standard deviation of each other.

Plasma treatments have no significant effect on  $G_{IIC}$  with E-Film interleaved composites.  $G_{IIC}$  increases five-fold with the use of the E-film interleaf.

Plasma treatment increases  $G_{IIC}$  for teflon film laminates. It is not possible to measure the  $G_{IIC}$  of the untreated teflon interleaved composite because the bond between the resin and the film is too weak. The  $G_{IIC}$  values of teflon treatment one and two are within a standard deviation of each other. Teflon treatment two is similar to

treatment one except the allylamine exposure time is increased 50%. The  $G_{IIC}$  value for teflon treatment three is approximately double the treatment one and two values.

Teflon plasma treatment conditions three and two are similar to kapton plasma treatment conditions two and one, respectively. However while the more severe plasma treatment doubles  $G_{IIC}$  in the teflon case, the  $G_{IIC}$  of kapton is essentially unchanged. This result is not surprising since the effect of different plasma treatments on the film surfaces will depend on the chemical structure of the polymer film. Thus optimization of treatment conditions is sensitive to film surface chemistry. The  $G_{IIC}$  of kapton interleaved composites may increase with plasma treatments in which either allylamine monomers possess a higher concentration of reactive groups or another monomer is used.

The locus of failure for ENF samples is determined with FTIR. ATR spectra of the interleaf side of ENF failure samples were examined. Figures 22 and 23 show ATR spectra of plasma treated films and the film side of failed ENF specimens with kapton and teflon interleaf films. These spectra indicate that the transmission valleys due to allylamine do not appear on the fractured samples. With both film materials failure occurs at the film-grafted polymer interface. These results demonstrate the importance of film adhesion in the fracture process with interleaved composites.

The ENF failure surfaces are also characterized with SEM. Figure 24 shows the ENF failure surface of a composite without an interleaf. With this material crack propagation energy is absorbed via resin fracture and fiber bridging. The  $G_{IIC}$  value of this composite is comparable to that of composites interleaved with untreated kapton. Figure 25 shows the failure surface of a composite interleaved with untreated kapton. With this material crack propagation energy is absorbed via film tearing. The fracture surface of plasma treated kapton interleaved composites (Figure 26) contains fewer sites of film tearing. However at these sites film deformation is more extensive. A limited number of hackles are evident on the interleaf surface. Thus even the addition of a brittle film as an interleaf material markedly increases the amount of crack propagation energy absorbed.

A similar failure surface topology is evident with the E-film interleaf (Figure 27). The hackles on the E-film are more elongated. This feature is evidence of increased ductility. Tensile tests show this film is slightly more ductile than the kapton film,

however, the critical crack propagation energy achieved with this film is five times that obtained with a kapton interleaf.

Since tensile test results on teflon show that there is extensive plastic deformation before failure, it seems reasonable to expect that the ENF failure surfaces of teflon interleaved composites would be characterized by extensive plastic deformation features. However, for teflon treatment two Figure 28 shows that there is limited deformation on the ENF failure surface. Viewing this region at a higher magnification, Figure 29 shows that on a local level the teflon definitely deforms during fracture. The effect of the more severe number three plasma treatment on plastic deformation of the teflon interleaf during mode two crack propagation is viewed in Figure 30. In this case the teflon interleaf deforms extensively. The contrast between the failure surface with treatment two (Figure 28) and treatment three (Figure 30) is marked and corresponds to the ENF test results of 208 and 392 J/m<sup>2</sup> for these treatments. This increase in energy absorption may be due to increased adhesion between the film and the resin.

It is interesting to note that film deformation by itself is not a sufficient determinant of interleaf effectiveness. Comparison of failure surface topologies shows that teflon film deforms much more than the kapton or E-films even though these films provide larger critical crack propagation energies. An explanation may be that the  $G_{IIC}$  of the interleaved composite is dependent on the toughness of the film material. If this explanation is valid, it is probable that improvements in the level of adhesion would produce limited additional increases in the composite fracture toughness with teflon interleafs.

## CONCLUSIONS

This study demonstrates that the material properties of the interleaf films selected are crucial. Even though plasma treated kapton fails in a brittle manner, when interleaved into a composite this film provides a marked improvement in critical crack propagation energy. The  $G_{IIC}$  improvements with the soft teflon film material are not as significant and may be limited by the film toughness.

This work demonstrates that film-resin adhesion can be increased through plasma treatment of interleaf films. Although the treatments presented here increase the

critical crack propagation energy of Cycom 3100/IM6 composites, evidence that the locus of failure in ENF testing is at the film-grafted polymer interface shows that plasma treatments can be improved to maximize film-resin adhesion. A high degree of adhesion between the film and the composite resin is a requirement to maximize fracture toughness in interleaved composites. A high level of film-resin adhesion is the probable cause for the large critical crack propagation energy achieved with the E-film interleaf.

Four test methods to measure film-resin adhesion were utilized in this work. Unfortunately all of these test methods are limited in ability to characterize film-resin adhesion. No one test method can be used for the full range of adhesive strength possibilities. The lap shear test is suitable when adhesion is low. Low to moderate bond strengths can be measured with flatwise tension testing. Moderate to high adhesive strengths can be determined with the floating-roller peel test. Clearly the need exists for a more universal measure of adhesive strength for interleaved composites.

Fracture toughness test results show that the fracture characteristics of a brittle composite can be significantly improved through interleaving. The addition of a brittle interleaf film such as plasma-treated kapton to a brittle BMI/graphite laminate doubles the critical crack propagation energy. Another brittle film, the E-film, which has greater film-resin adhesion, increases the critical crack propagation energy fourfold when used as an interleaf material.

A general approach for the development of novel interleaved composites should entail selection of films with high toughness followed by plasma tailoring of surface characteristics for adhesion to the matrix of interest. Surface treatments which will provide optimum interleaf performance should focus on film-resin adhesion characteristics. An optimum interleaf material is a tough film with a film-resin adhesive strength greater than the composite's interlaminar shear strength.

## REFERENCES

1. Williams, J.G., and Rhodes, M.D., Williams et al, Special Technical Publication 787, American Society for Testing and Materials, Philadelphia, 1983.
2. Riew, C.K., and Gillham J.K., *Rubber-Modified Thermoset Resins*, Advances in Chemistry Series 208, American Chemical Society, Washington, D.C., 1984.
3. Turpin, R.L. and Green, A.L., 35th SAMPE Symposium and Exhibition, Society for the Advancement of Process and Materials Engineering, Covina, Ca., 1990, pp. 1079-1088.
4. Ko, F.K., Textile Structural Composites, eds. T.W. Chow and F.K. Ko, Elsevier Science, Netherlands, 1989, pp. 129-171.
5. Dolan, G.L. and Masters, J.E., 20th International SAMPE Technical Conference, Society for the Advancement of Process and Materials Engineering, Covina, Ca., 1988, pp. 34-45.
6. Kreiger, R.B. 29th SAMPE Symposium and Exhibition, Society for the Advancement of Process and Materials Engineering, Covina, Ca., 1984, pp. 1570-1584.
7. Evans, J.E. and Masters, J.E., Toughened Composites, ASTM STM 937, ed. N. Johnston, American Society for Testing and Materials, Philadelphia, 1987, pp. 413-436.
8. Masters, J.E., Courter, J.L., and Evans, R.E., 31st International SAMPE Symposium and Exhibition, Society for the Advancement of Process and Materials Engineering, Covina, Ca., 1986, pp. 844-858.
9. Armstrong-Carroll, E. and Donnellan, T.M., 1990 Materials Congress, American Society of Civil Engineers, New York, 1990.
10. Armstrong-Carrol, E. Iskandarani, B., Kamel, I., and Donnellan, T., ASTM Fourth Symposium on Composite Materials: Fatigue and Fracture Conference Proceedings, May 1991.

**NAWCADWAR-92102-60**

11. Armstrong-Carrol, E. and Donnellan, T., Second Navy R&D Information Exchange Conference, April, 1991.
12. Masters, J.E., Interlaminar Fracture of Composites, ed. E.A. Armanios, Trans Tech Publications, Switzerland, 1989, pp. 317-347.
13. Wertheimer, M.R. and Schreiber, H.P., Journal of Applied Polymer Science, Vol. 26, 1981, pp. 2087-2096.
14. Petrie, E.M. and Chottiner, J.C., 40th Annual SPE Technical Conference and Exhibition: ANTEC 82, Society of Plastics Engineers, St. Louis, Mo., 1982, pp. 777-779.
15. Krishnamurthy, V., Kamel, I.L., and Wei, Y., Journal of Polymer Science, Part A, Vol. 27, 1989, pp. 1211-1224.
16. Miller, R.N., Humphrey, F.T., and Bleich A., *Cleaning and Chemical Treatment of Aircraft Surfaces to Provide Optimum Cleaning Properties*, Final Report NAVAIR Contract #N00019-68-C-0017, 1970.



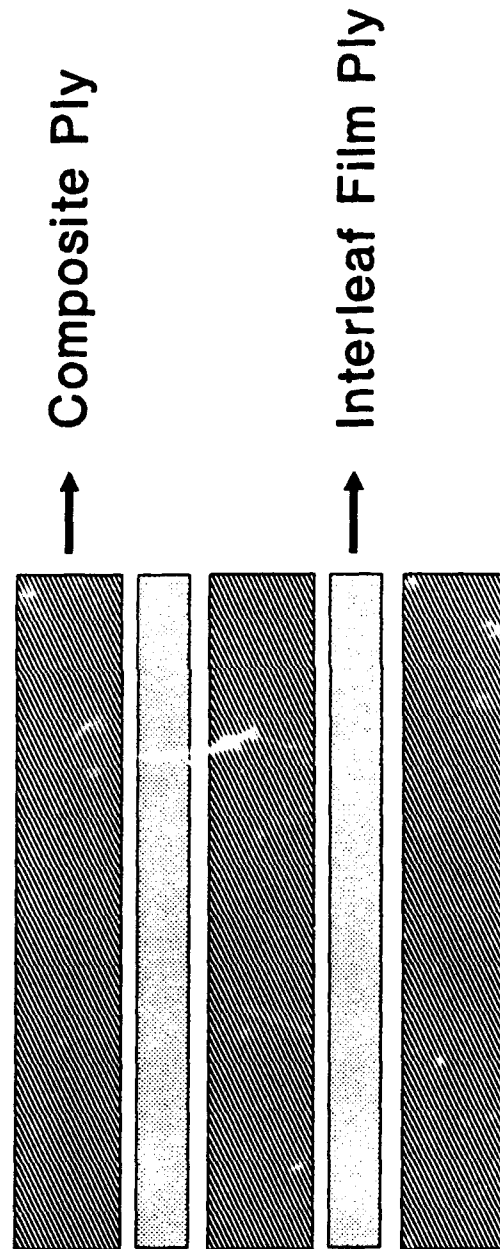


Figure 1. Illustration Of The Interleaving Concept.

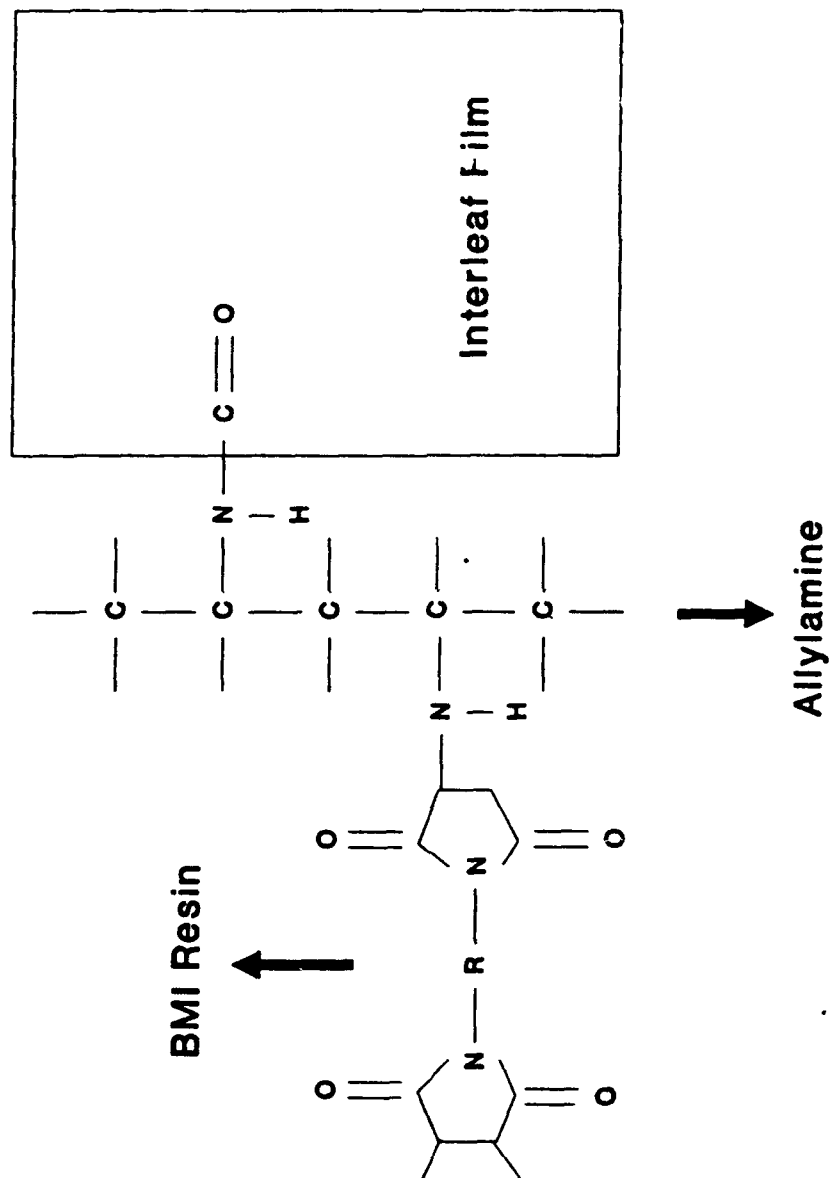


Figure 2. Possible Interleaf Film-Resin Bonding Mechanisms. Schematic Depicts How Grafted-Allylamine Polymer Acts As A Coupling Agent Between The Interleaf Film And BMI Resin.

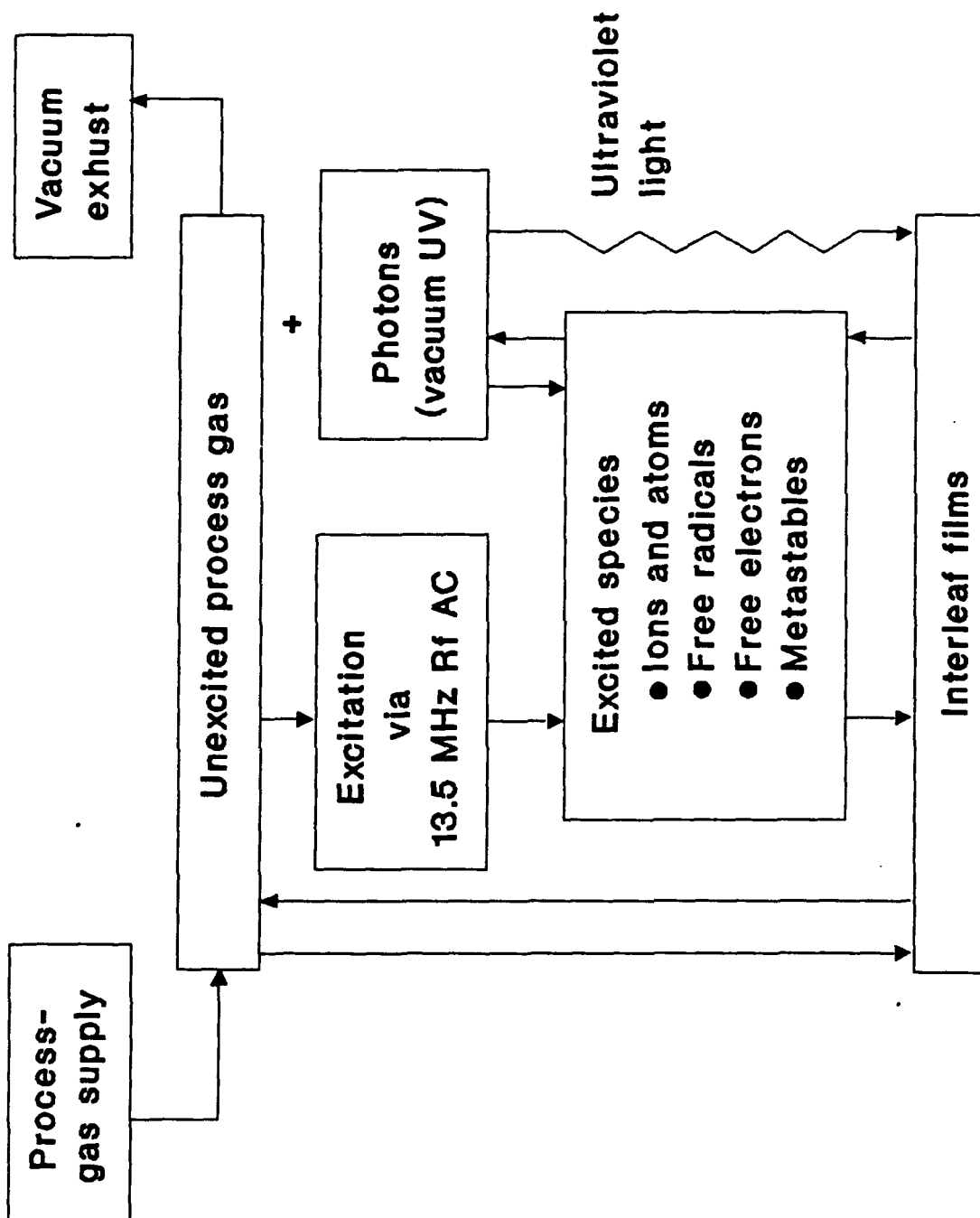
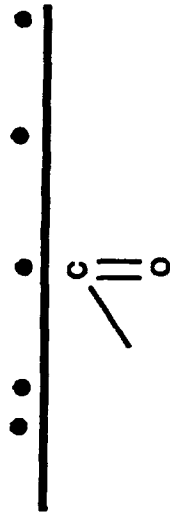
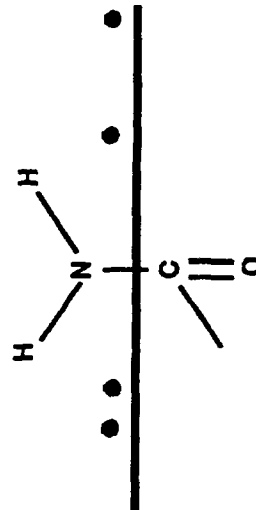


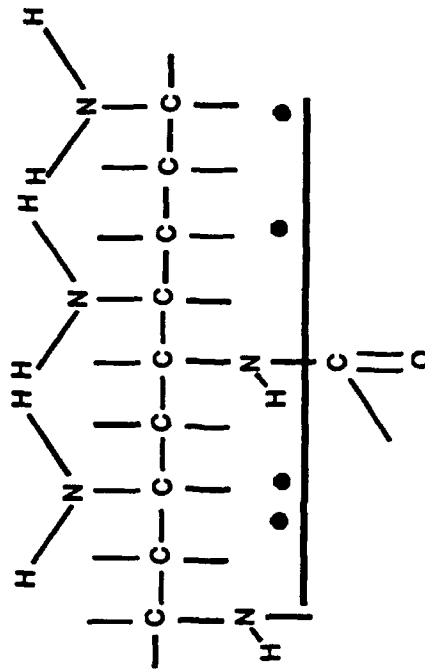
Figure 3. Schematic Of The Process Through Which Process Gases Are Excited And Deposited On The Interleaf Films.



Argon treatment



Ammonia treatment



Allylamine treatment

Figure 4. Possible Surface Chemistries Produced With Argon, Ammonia, And Allylamine Plasma Treatments. The Filled Circles Represent Carbonyl Free Radicals Formed During Plasma Treatment.

NAWCADWAR-92102-60

Table 1.  
Interleaf Film Plasma Treatments.

Sample	Argon			Subsequent		
	Power (w)	Pressure (T)	Time (min)	Power (w)	Pressure (T)	Time (min)
Kapton ammonia treatment one	30	0.5	5	30	0.5	5
Kapton ammonia treatment two	30	0.5	5	30	0.5	10
Kapton ammonia treatment three	100	0.5	10	100	1.0	45
Kapton allylamine treatment one	50	0.5	10	70	0.8	30
Kapton allylamine treatment two	150	0.7	15	100	0.7	50
Kapton allylamine treatment three	50	0.5	5	50	0.5	5
Kapton allylamine treatment four	50	0.5	5	50	0.5	7
Kapton allylamine treatment five	50	0.5	5	50	0.5	10
Kapton allylamine treatment six	50	0.5	10	70	0.7	20
Kapton allylamine treatment seven	50	0.5	10	30	0.7	20
Kapton allylamine treatment eight	50	0.5	10	50	0.7	10
Kapton allylamine treatment nine	50	0.5	10	50	0.7	20
E-film allylamine treatment one	50	0.5	15	50	0.6	30
E-film allylamine treatment two	70	0.5	30	70	1.0	30
Teflon allylamine treatment one	50	0.5	10	70	0.8	20
Teflon allylamine treatment two	50	0.5	10	70	0.8	30
Teflon allylamine treatment three	150	0.7	15	100	0.7	50

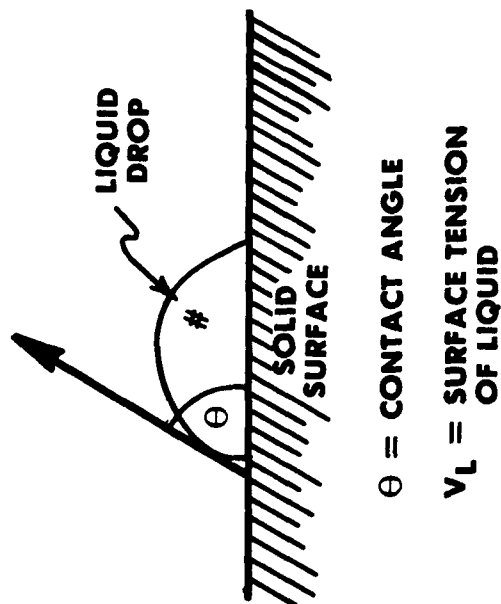
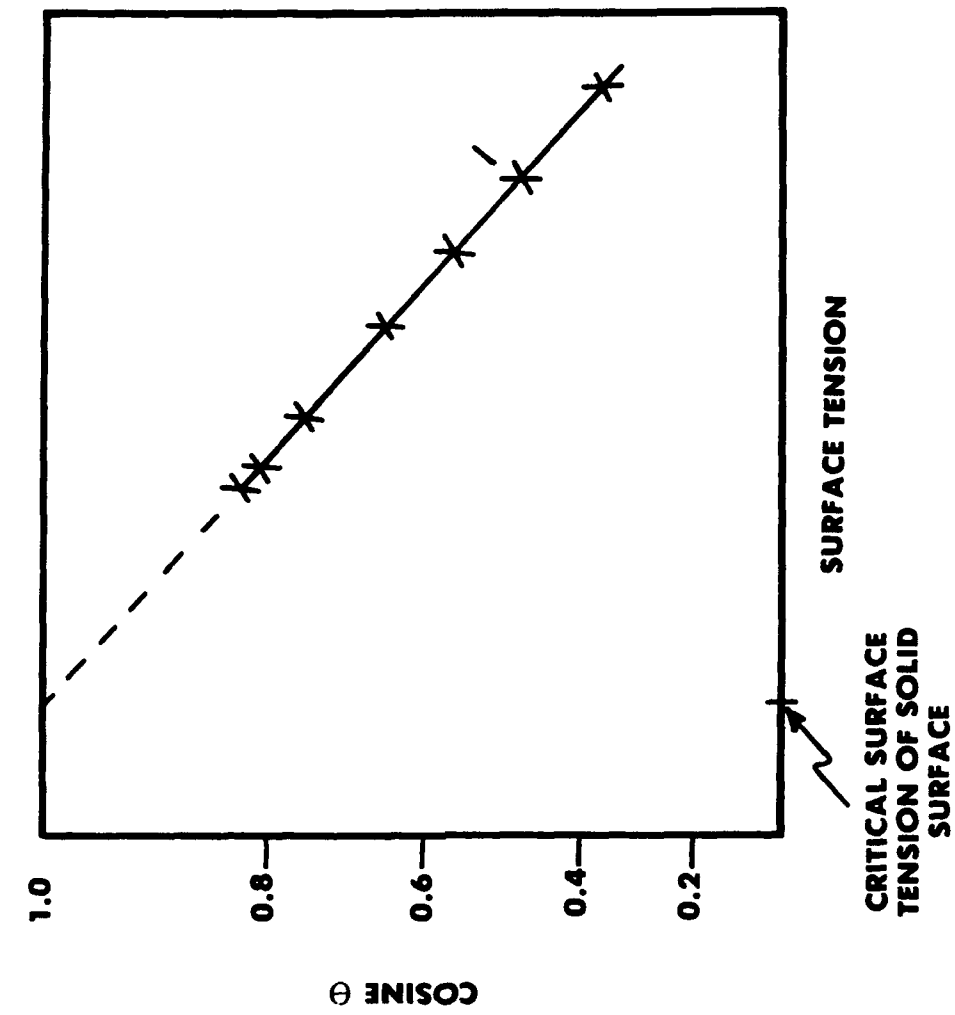


Figure 5. Illustration Of How Contact Angle Is Measured And Critical Surface Tension Is Determined.

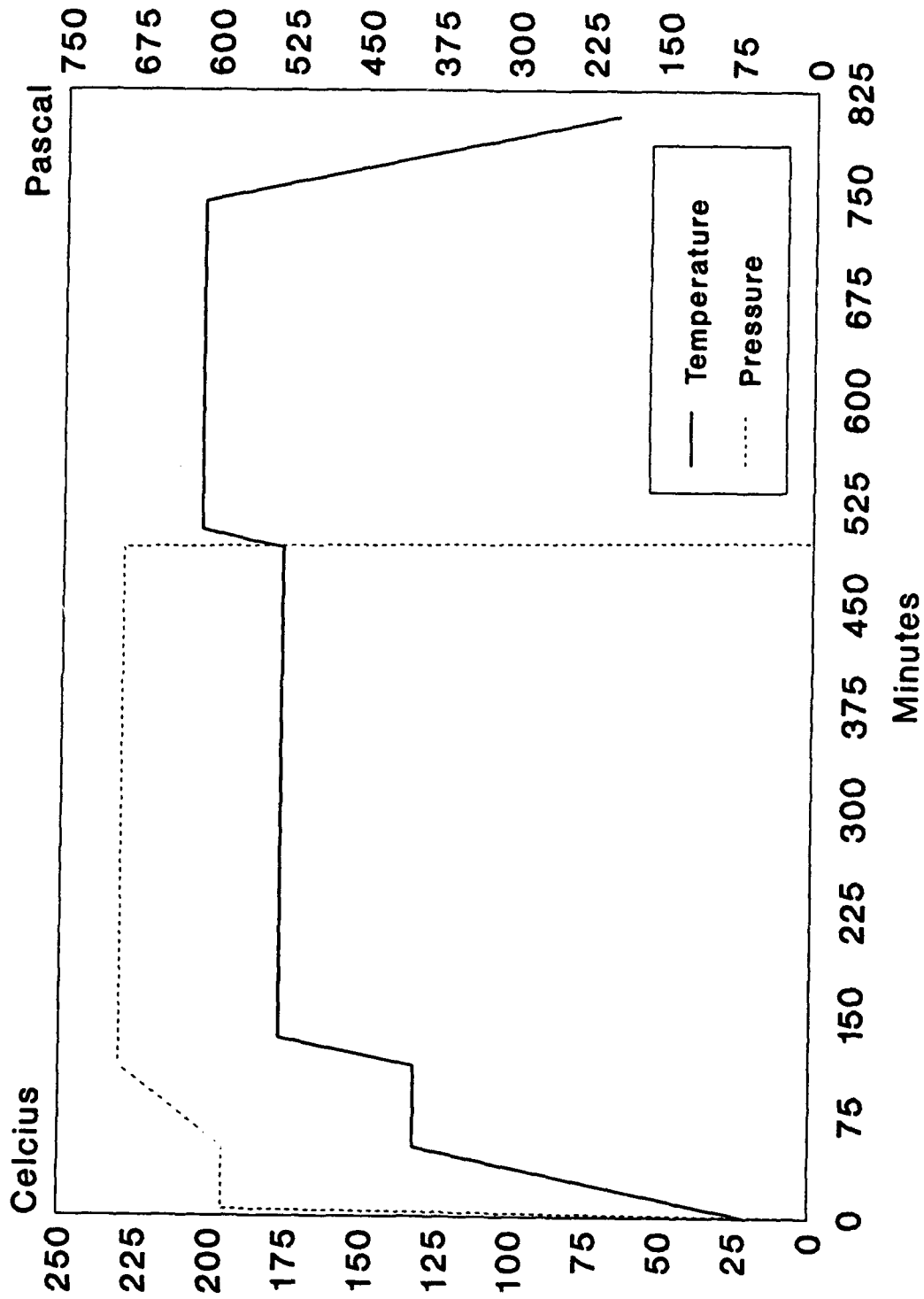


Figure 6. Processing Cycle For Interleaved Cycrom 3100/IM6.

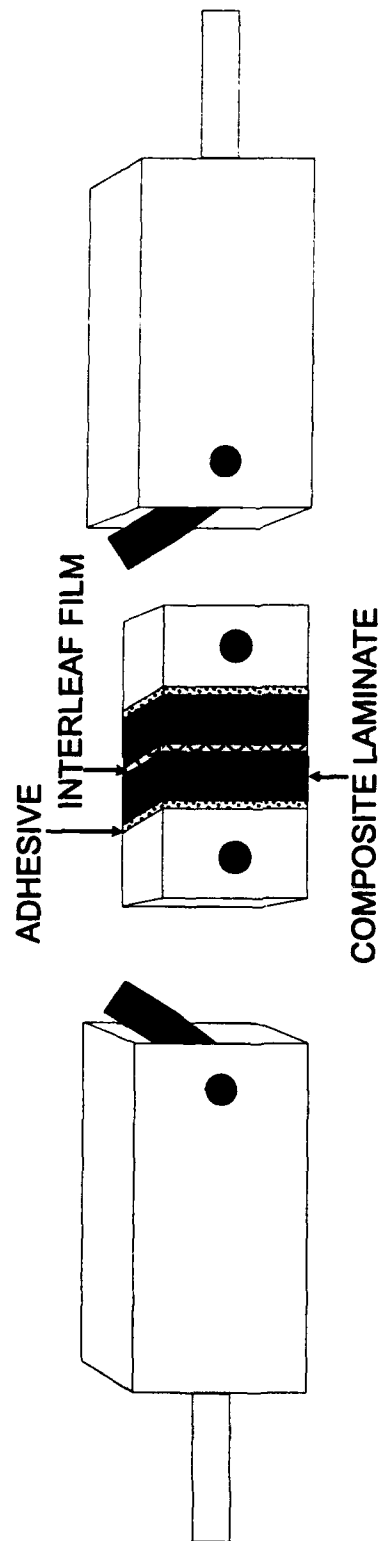


Figure 7. Schematic Of The Flatwise Tension Test Set-Up.



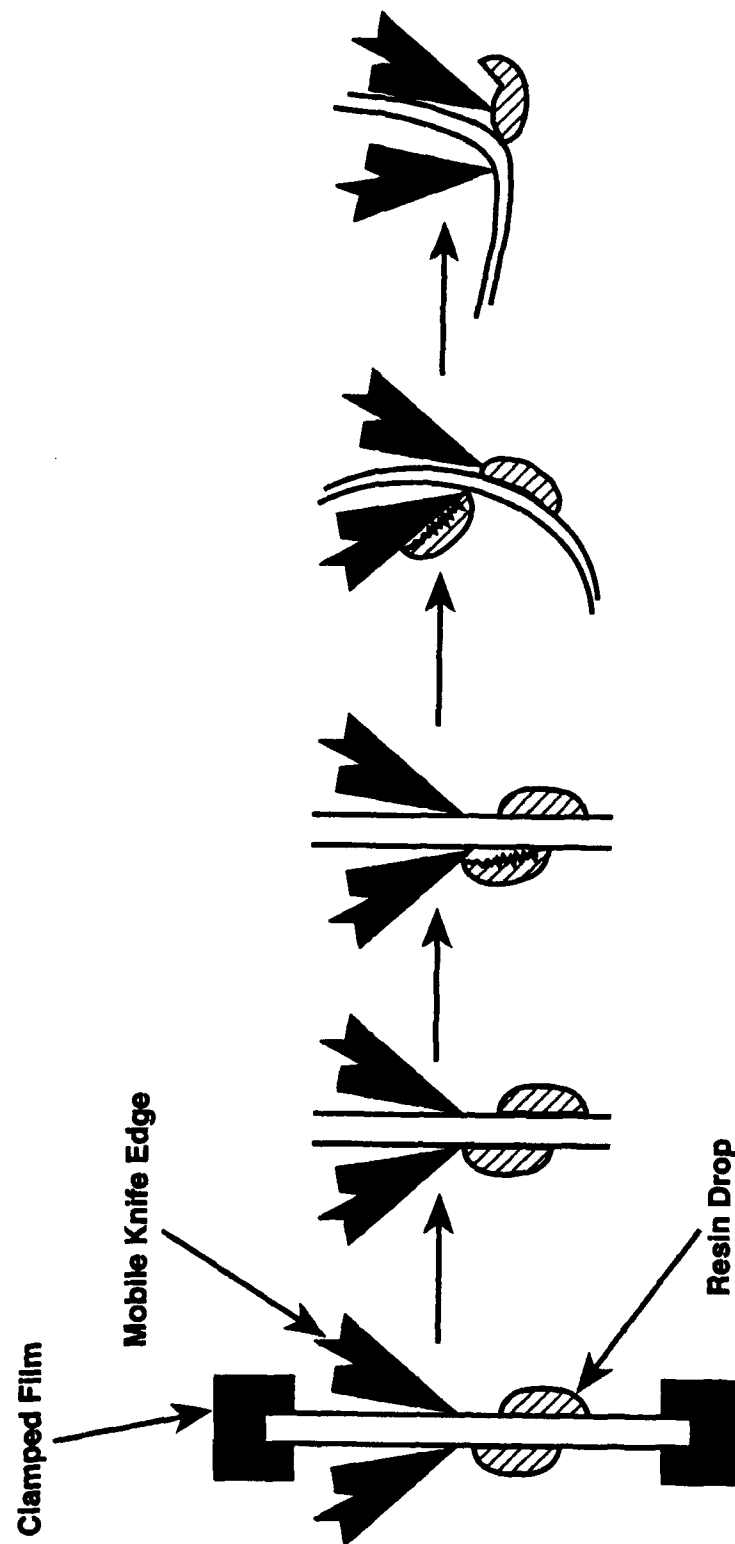


Figure 8. Depiction Of The Typical Test Sequence For The Resin-Drop Shear Test.

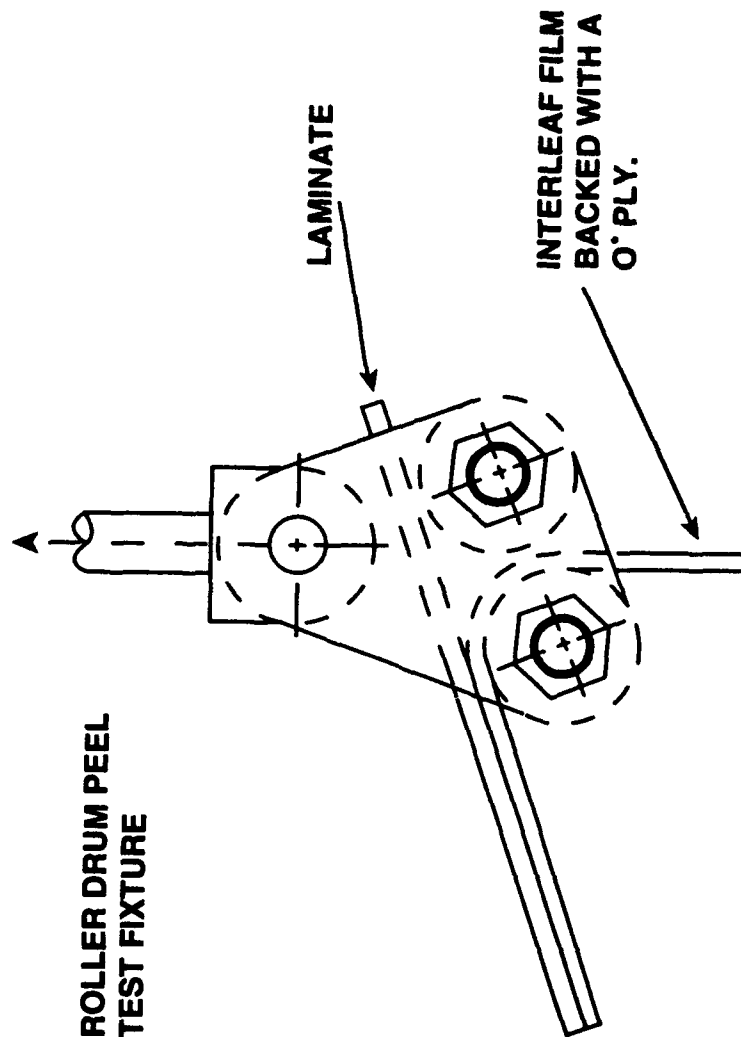


Figure 9. Schematic Of The Floating Roller Peel Test Set-Up.

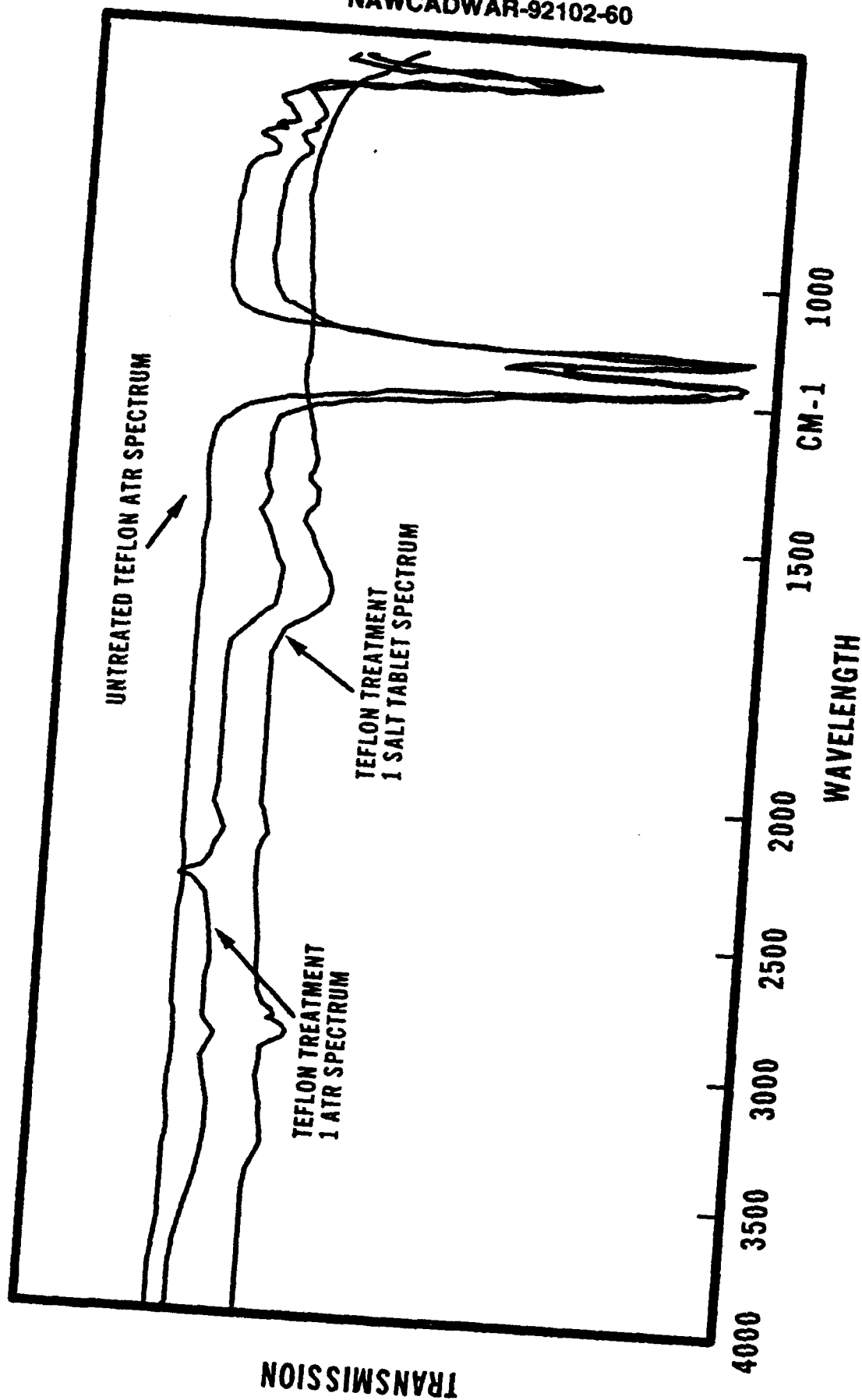


Figure 10. Transmission Spectra Of Untreated And Plasma Treatment One Teflon. Three Allylamine Valleys Are Visible On Spectra Of Plasma Treated Teflon Collected From A Salt Tablet And An ATR Crystal At  $3000\text{cm}^{-1}$ ,  $2100\text{cm}^{-1}$ , And  $1600\text{cm}^{-1}$ .

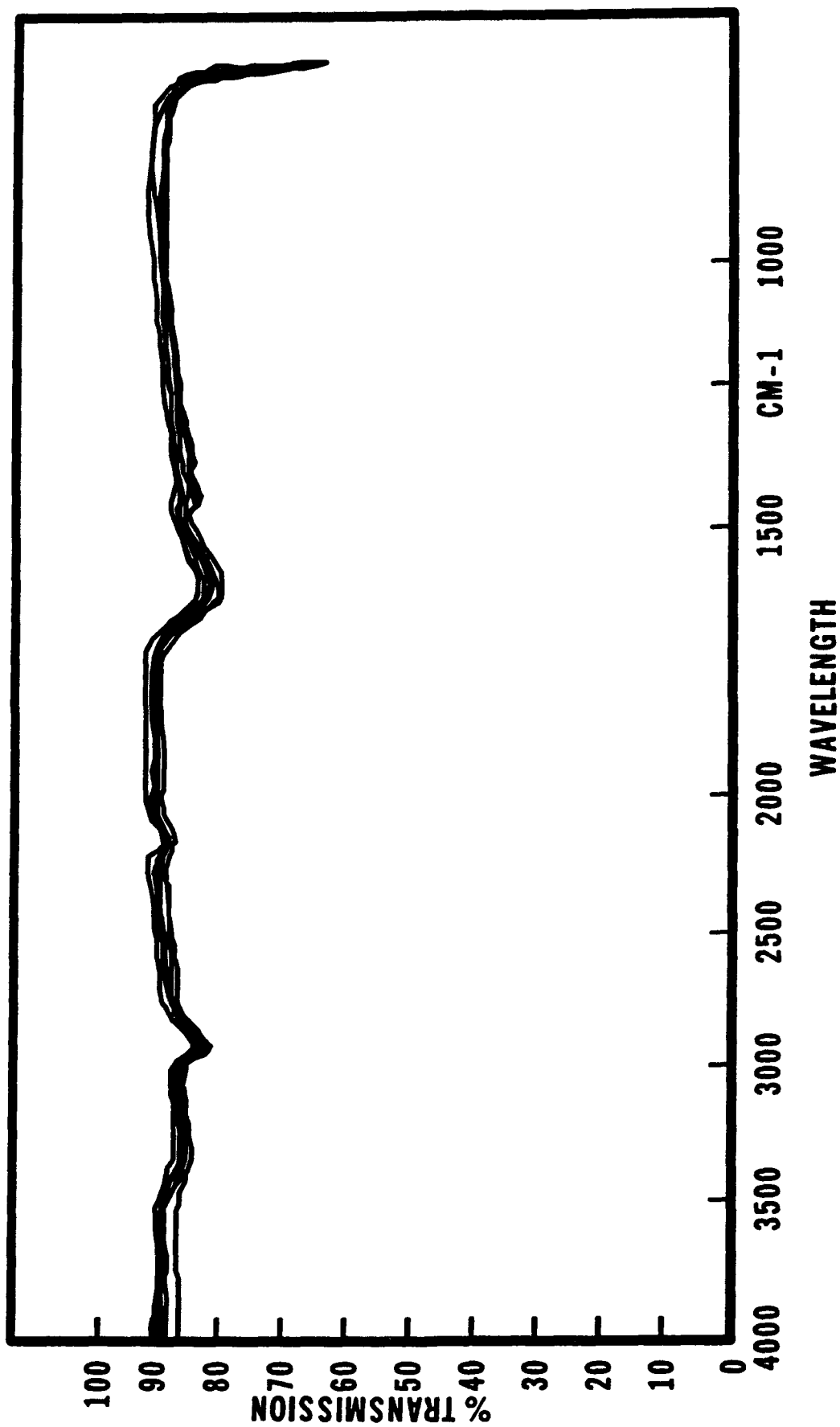


Figure 11. Reproducibility Of Plasma Treatments As Collected With Salt Tablets Placed In The Plasma Reactor During Film Treatment. Seven Different Batches Of Teflon Treatment One Are Plotted.

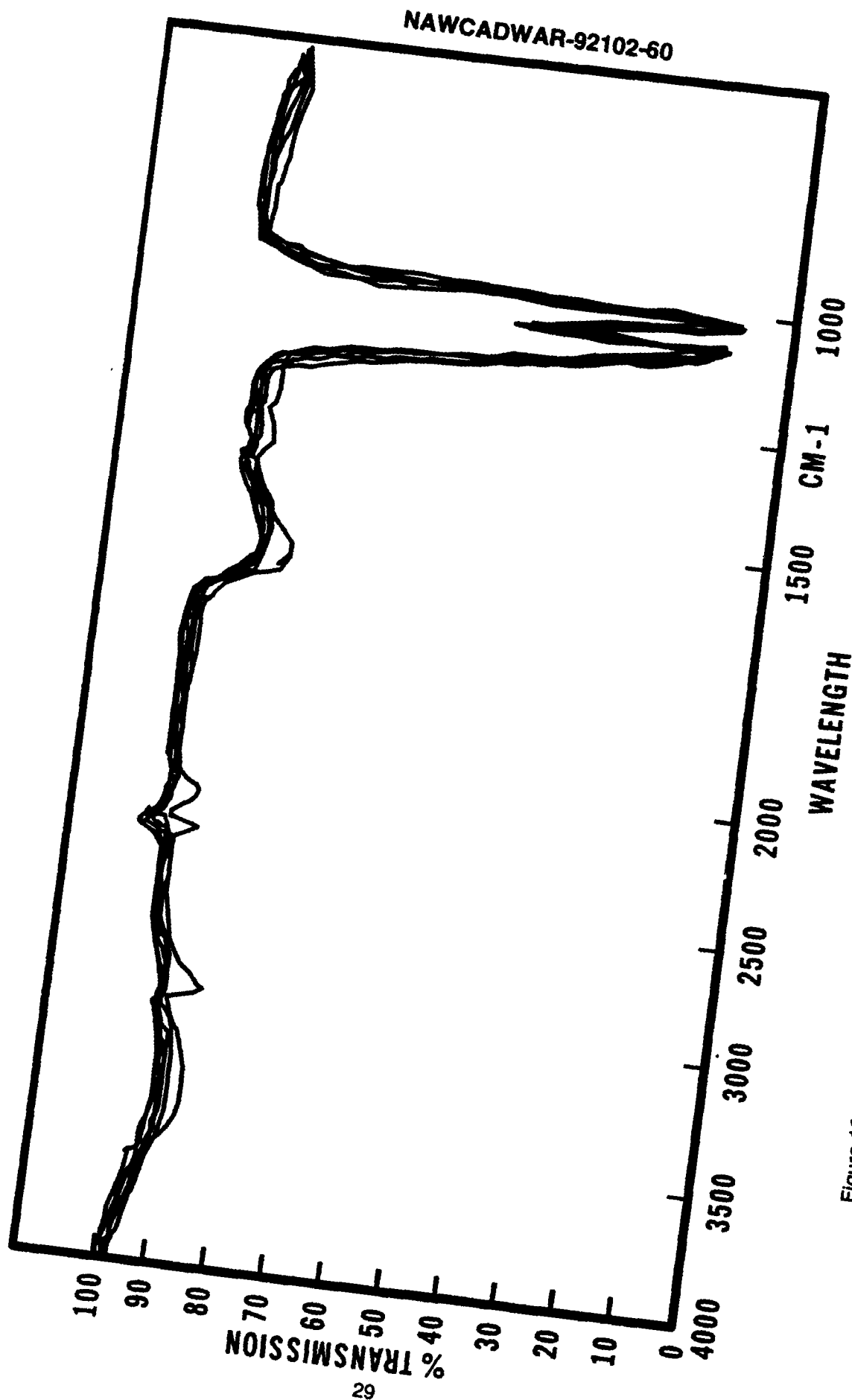


Figure 12. Reproducibility Of Plasma Treatments As Collected With ATR Spectra Of Treated Films.  
Five Different Regions Of A Teflon Treatment One Film Are Plotted.

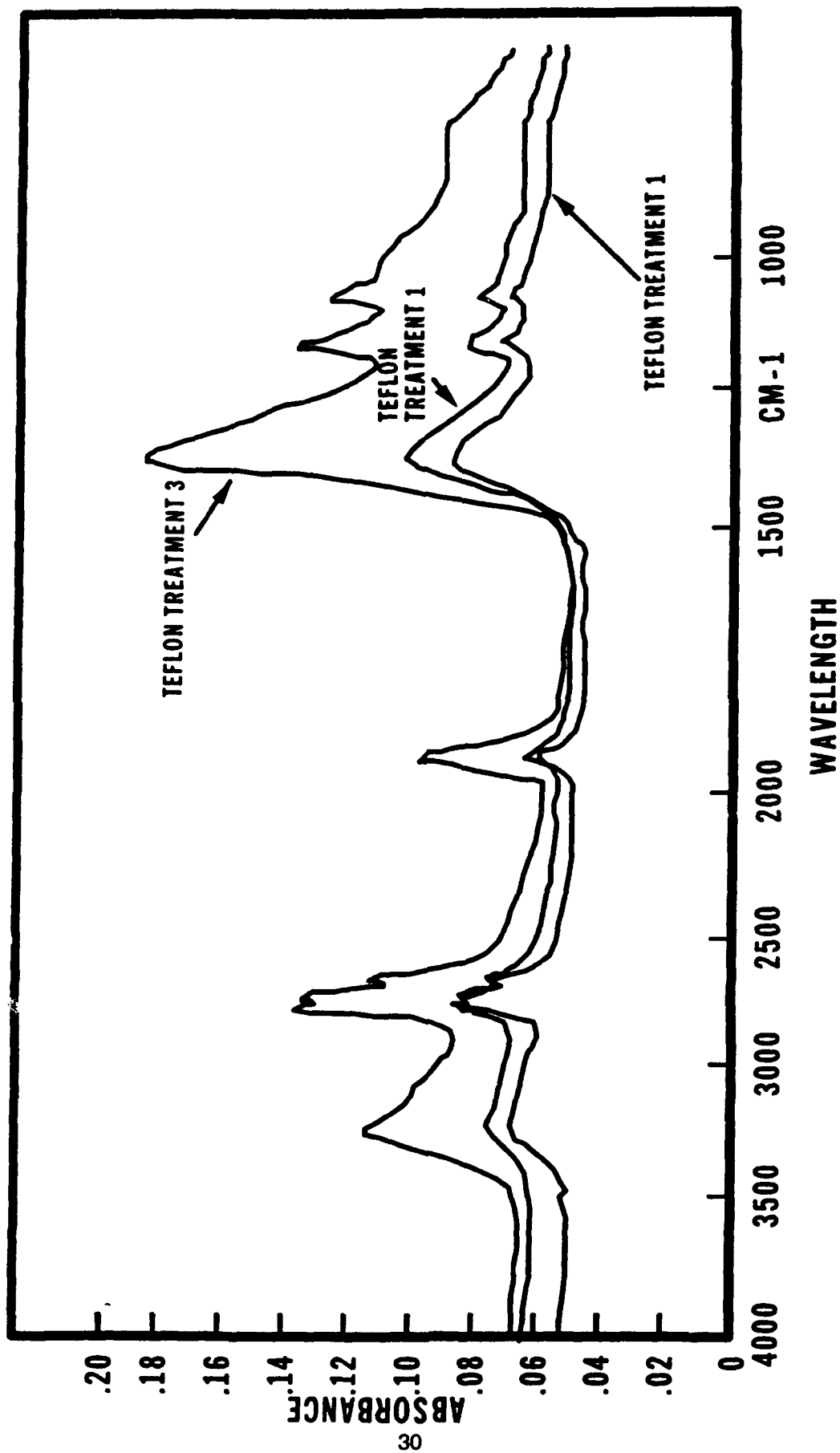


Figure 13. Absorption Spectra Of Plasma Treated Teflon. The Differences In Peak Intensity Due To The More Severe Plasma Treatment Are Greater Than Those Due To Variations In Reproducibility.

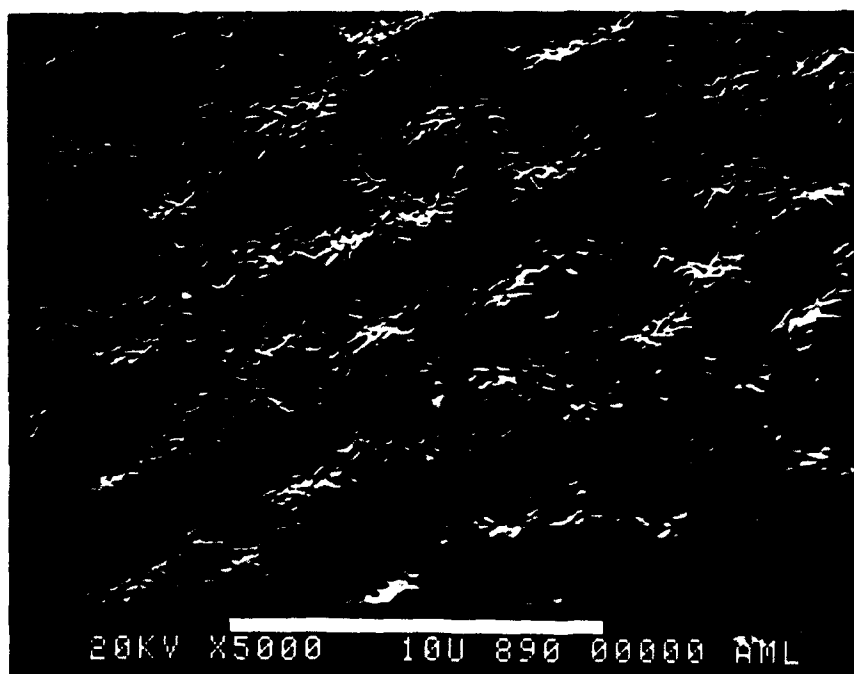


Figure 14. Untreated Teflon Film. Topography Is Marked By A Dendritic Structure.

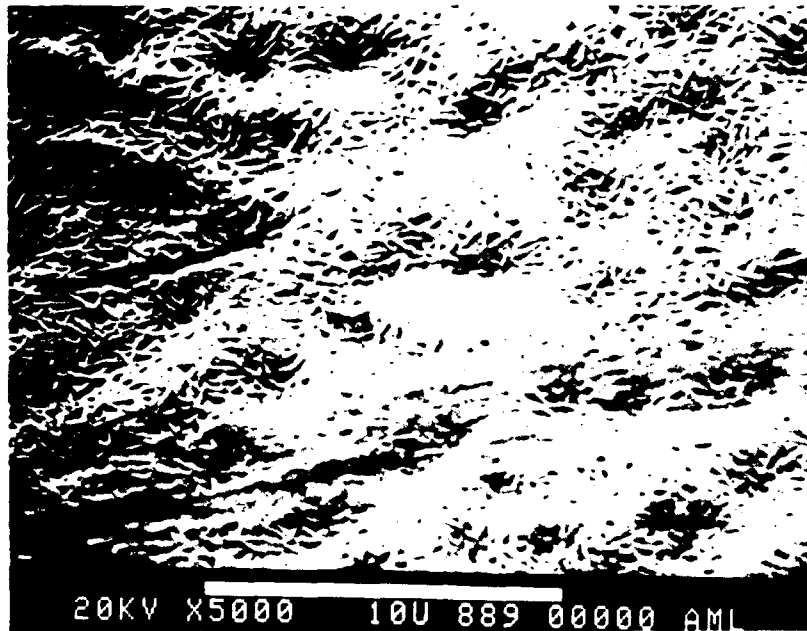


Figure 15. Teflon Film Treated With Treatment Two. Valleys In Film Topography Are Partially Obscured By Grafted Allylamine.

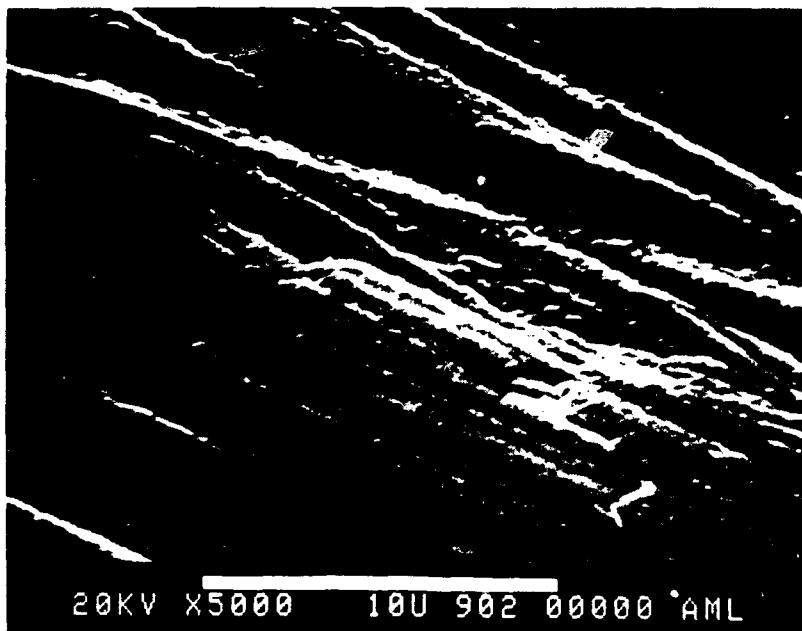


Figure 16. Teflon Film Treated With Treatment Three. Original Teflon Topography Is Totally Obscured By Plasma Treatment.



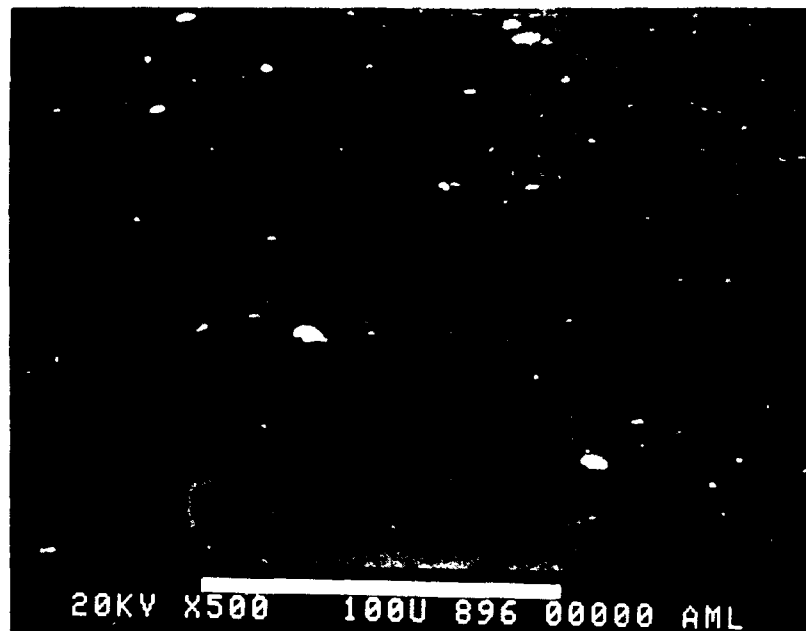


Figure 17. Kapton Film Treated With Treatment Two.  
Similar To Untreated Kapton Film Topography.



Figure 18. Untreated Kapton Film Failed In Tension. Failure Surface Is Featureless.

NAWCADWAR-92102-60

Table 2.  
Tensile Properties Of Interleaf Films.

Sample	Elastic Limit			Failure	
	Stress (MPa)	Strain (cm/cm)	Modulus (MPa)	Stress (MPa)	Strain (cm/cm)
Kapton untreated	56	0.02	2830	202	0.44
Kapton treatment two	38	0.01	3377	176	0.54
Teflon untreated	13	0.90	14	31	5.90
Teflon treatment two	15	0.03	462	29	2.86
Teflon treatment three	17	0.03	681	22	0.82
E-film untreated	97	0.03	1743	161	0.45

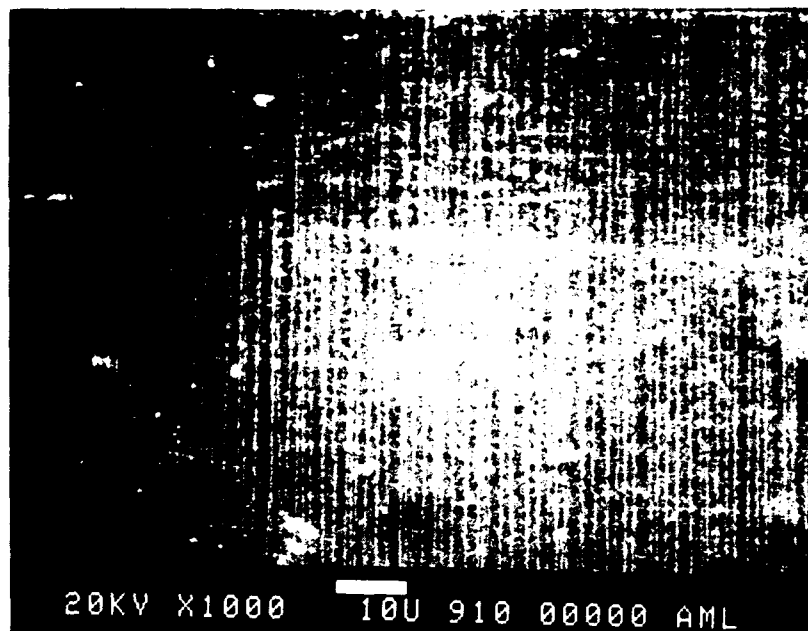


Figure 19. Kapton Film Treatment Two Failed In Tension.  
Failure Surface Possesses Several Vertical Cleavage Striae.

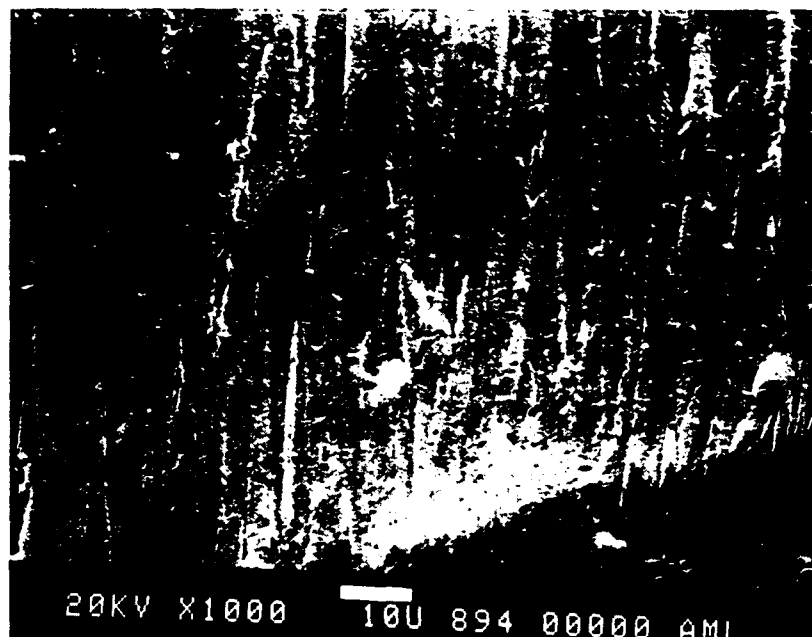


Figure 20. Untreated Teflon Film Failed In Tension. Outer Film Layers Deform And Tear Away From Film. Material Behaves In This Manner Since It Is Composed Of Several Thin Cast-Teflon Layers.

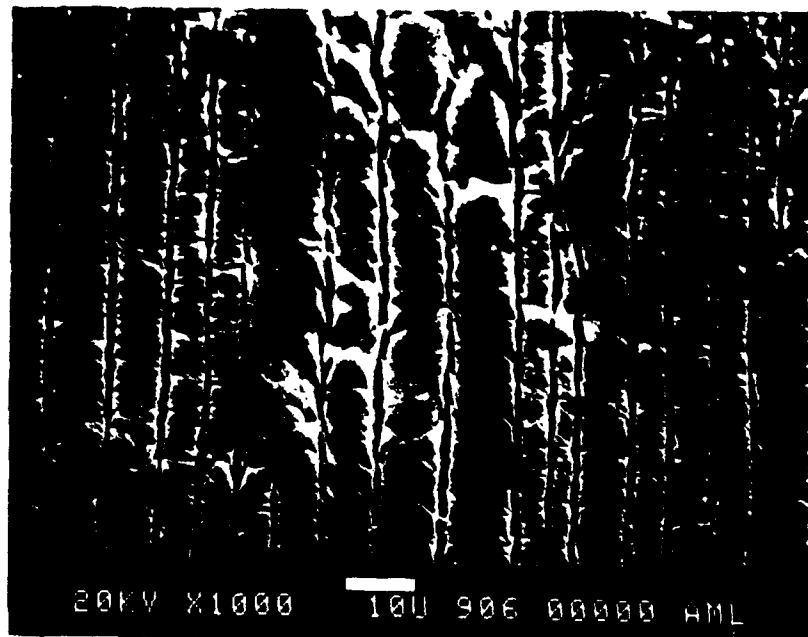


Figure 21. Teflon Film Treatment Three Failed In Tension Failure Surface Marked By Several Vertical Cleavage Striae. Within Each Stria The Failure Surface Is Cleaved At Several Locations.

NAWCADWAR-92102-60

Table 3.  
Peel Test Results.

Sample	Peel Strength (piw)
Kapton untreated . . . . .	0.1
Kapton allylamine treatment two . . . . .	0.1
Kapton allylamine treatment six . . . . .	0.1
Kapton allylamine treatment seven . . . . .	0.1
Kapton allylamine treatment eight . . . . .	0.8
E-film untreated . . . . .	6.5
E-film allylamine treatment one . . . . .	60.
E-film allylamine treatment two . . . . .	6.0
Teflon untreated . . . . .	0.0
Teflon allylamine treatment one . . . . .	0.4
Teflon allylamine treatment two . . . . .	1.0

**NAWCADWAR-92102-60**

**Table 4.  
ENF Test Results.**

<b>Sample</b>	<b>G2c (J/m<sup>2</sup>)</b>
Control .....	468
Kapton untreated .....	476
Kapton ammonia treatment one .....	630
Kapton ammonia treatment two .....	771
Kapton ammonia treatment three .....	806
Kapton allylamine treatment one .....	1016
Kapton allylamine treatment two .....	844
Kapton allylamine treatment three .....	928
Kapton allylamine treatment four .....	578
Kapton allylamine treatment five .....	595
E-Film untreated .....	1996
E-Film allylamine treatment one .....	1786
E-film allylamine treatment two .....	2084
Teflon untreated .....	0
Teflon allylamine treatment one .....	189
Teflon allylamine treatment two .....	208
Teflon allylamine treatment three .....	392

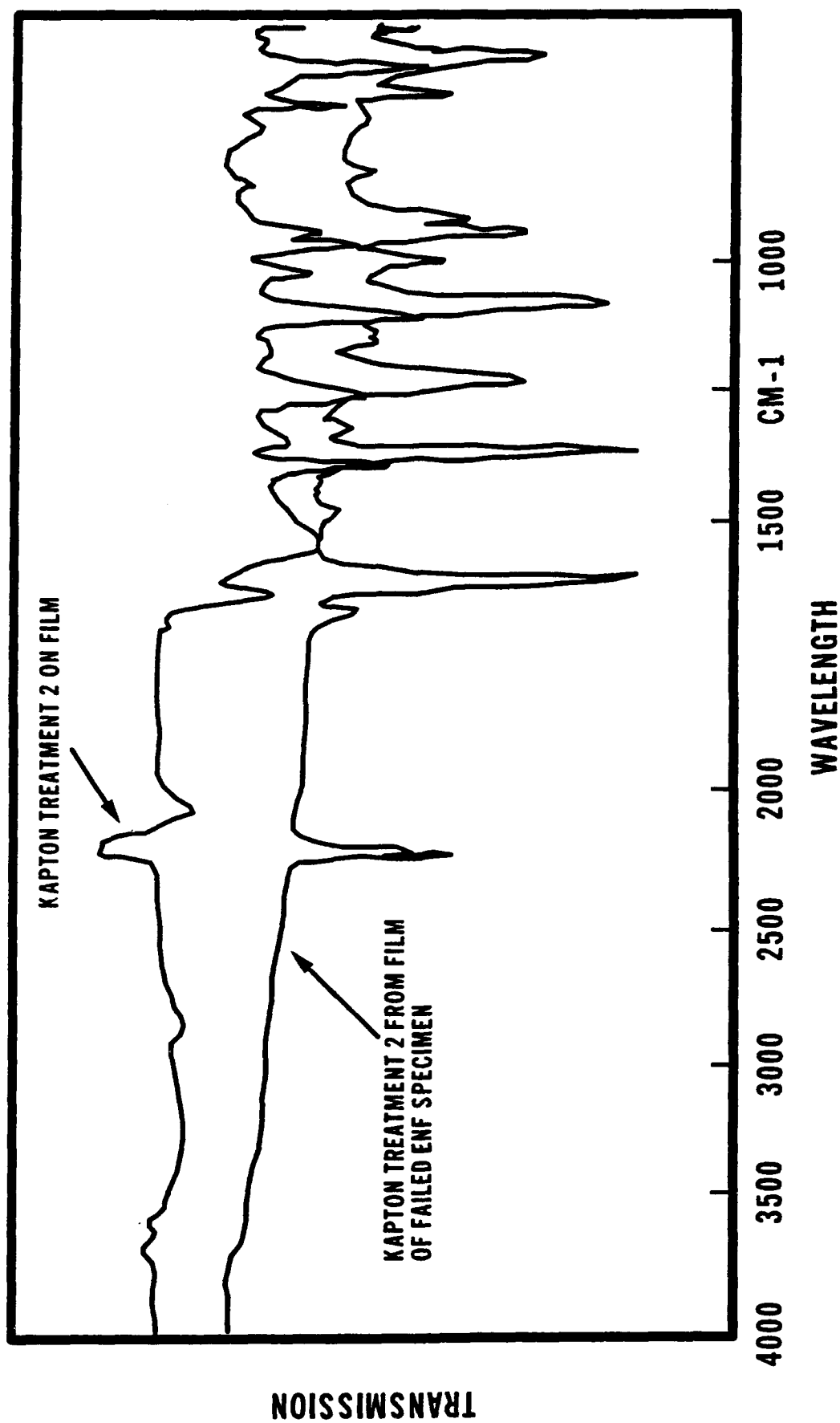


Figure 22. Spectrum Of An ENF Failure Surface Compared With Spectrum Of A Plasma Treated Film For Kapton Treatment Two. Allylamine Valleys Are Absent On The ENF Failed Film Surface.

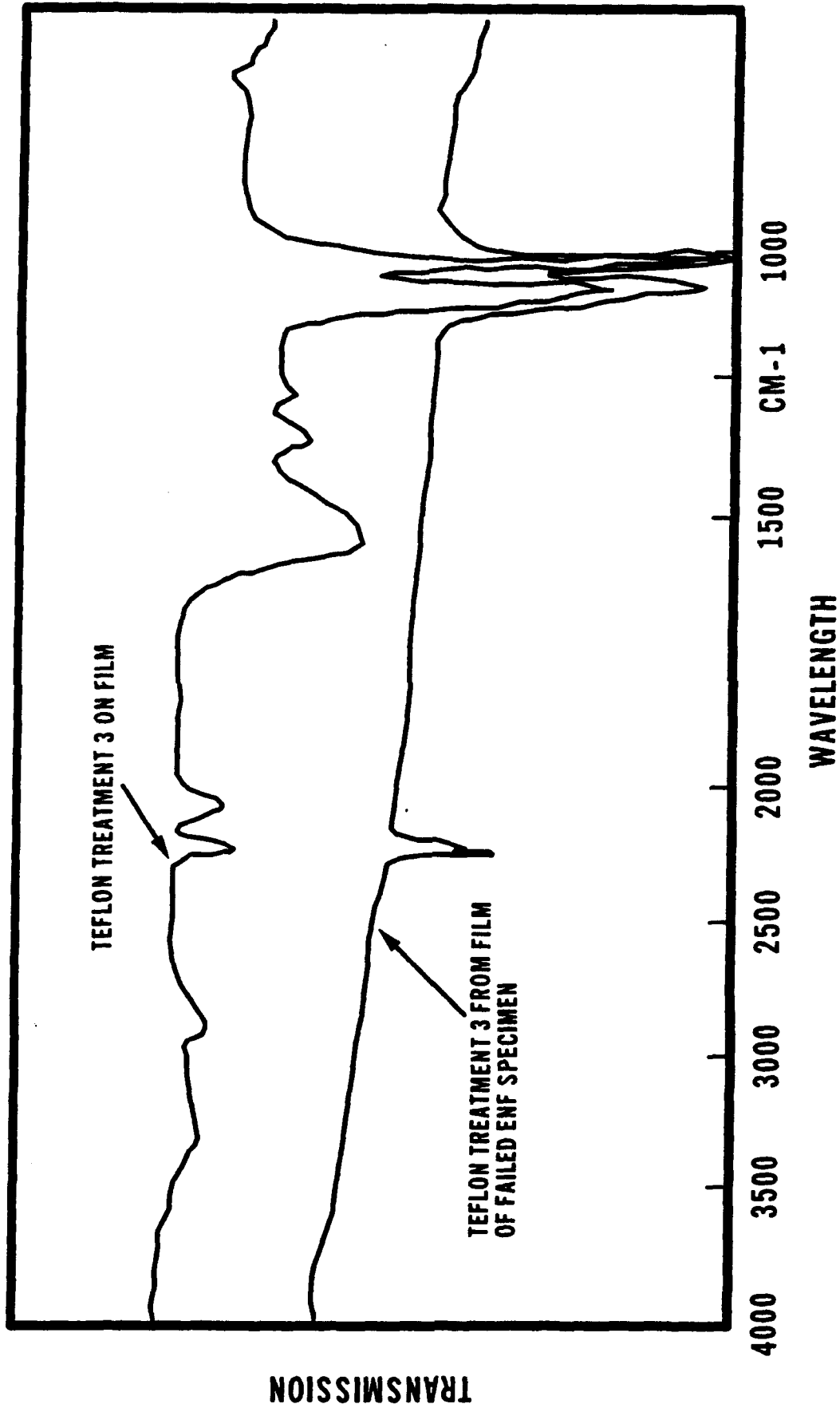


Figure 23. Spectrum Of ENF Failure Surface Compared With Spectrum Of Plasma Treated Film For Teflon Treatment Three.  
Allylamine Valleys Are Absent On The ENF Failed Film Surface.





Figure 24. Cycom 3100/IM6 Composite Failed Through ENF Testing.  
Fracture Energy Absorbed Through Resin Fracture.



Figure 25. Cycom 3100/IM6 Composite, Interleaved With Kapton Failed Through ENF Testing.  
Additional Fracture Energy Absorbed Through Film Tearing.

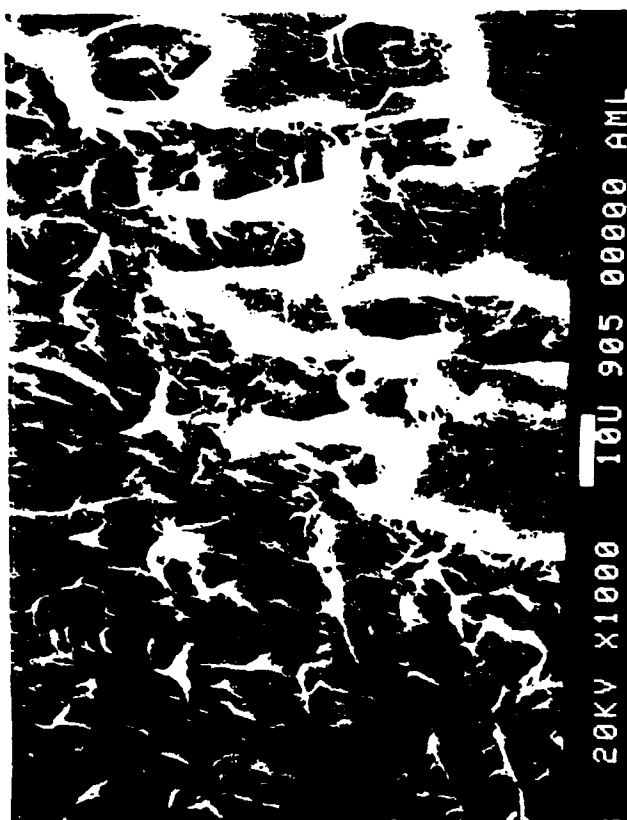


Figure 26. Cycom 3100/IM6 Composite, Interleaved With Kapton Treatment Two, Failed Through ENF Testing. More Deformation Is Evident At Film Tearing Sites. Some Hackles Are Evident.

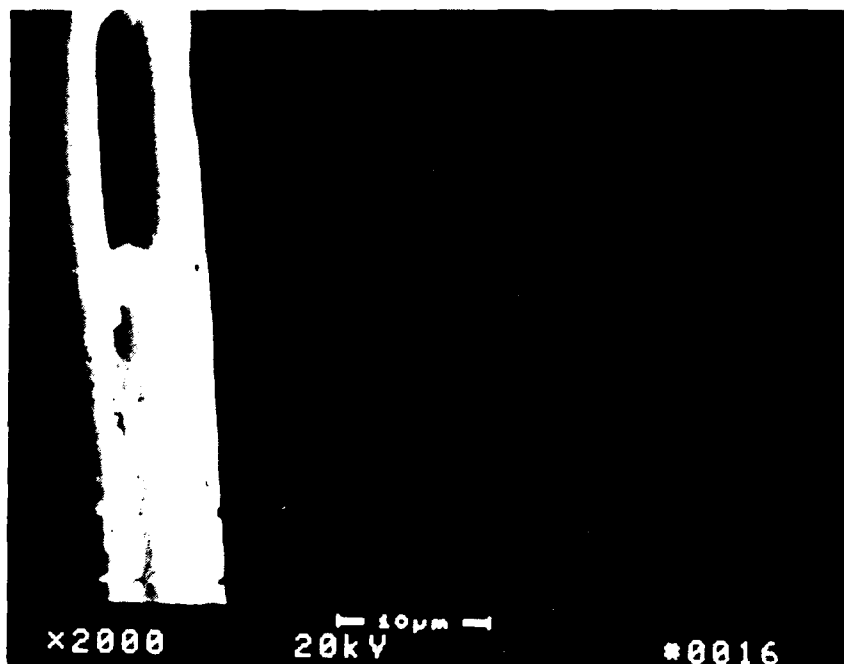


Figure 27. Cycom 3100/IM6 Composite, Interleaved With E-Film, Failed Through ENF Testing. Film Tears And Deforms. Hackle Possesses Ductile Features.



Figure 28. Cycom 3100/IM6 Composite, Interleaved With Teflon Treatment Two, Failed Through ENF Testing. Plastic Deformation Is Subtle.

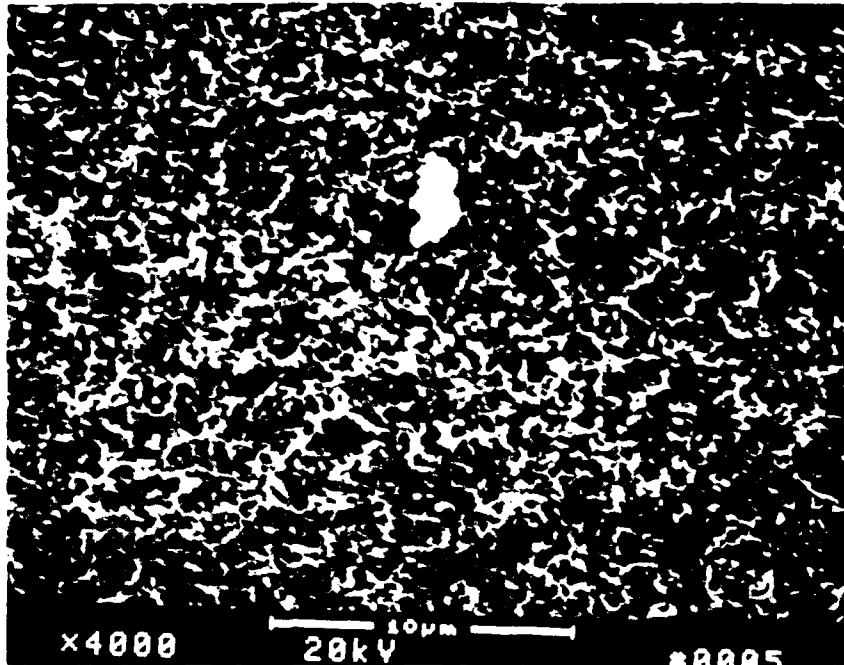


Figure 29. Cycom 3100/IM6 Composite, Interleaved With Teflon Treatment Two, Failed Through ENF Testing. Cratered Surface Denotes Extensive Local Deformation Of Teflon Film.



Figure 30. Cycom 3100/IM6 Composite, Interleaved With Teflon Treatment Three, Failed Through ENF Testing. Extensive Tearing and Stretching Of Teflon Film.

**DISTRIBUTION LIST (Continued)**  
Report No. NAWCADWAR-92102-60

	No. of Copies
Commanding Officer .....	1
Naval Air Warfare Center	
Aircraft Division Warminster	
Attn: Mr. I.S. Shaffer, Code 606	
P.O. Box 5152	
Warminster, PA 18974-0591	
Commanding Officer .....	10
Naval Air Warfare Center	
Aircraft Division Warminster	
Attn: R.E. Trabocco, Code 6064	
P.O. Box 5152	
Warminster, PA 18974-0591	
Commanding Officer .....	2
Naval Air Warfare Center	
Aircraft Division Warminster	
Attn: Code 8131	
P.O. Box 5152	
Warminster, PA 18974-0591	

**DISTRIBUTION LIST (Continued)**  
Report No. NAWCADWAR-92102-60

	No. of Copies
Commander .....	1
Naval Air Systems Command	
Attn: AIR-530	
Washington, DC 20361	
 Commander .....	 1
Naval Air Systems Command	
Attn: AIR-5304, AIR-5304C	
Washington, DC 20361	
 Commander .....	 1
Naval Air Systems Command	
Attn: AIR-530T	
Washington, DC 20361	
 Lockheed Engineering and Sciences Company .....	 1
Attn: Dr. John Masters	
c/o NASA Langley Research Center, M/S 188E	
144 Research Drive	
Hampton, VA 23666	
 Commander .....	 1
Naval Sea Systems Command	
Attn: SEA-05R	
Washington, DC 20362-5101	
 Commanding Officer .....	 1
Naval Ship Engineering Center	
Attn: NSEC 6101E	
Arlington, VA 20360	
 Commander .....	 1
Naval Surface Warfare Center	
Carderock Division, Annapolis Detachment	
Attn: E.T. Camponeschi, Code 2844	
Annapolis, MD 21402	
 Commanding Officer .....	 1
Naval Air Warfare Center	
Aircraft Division Warminster	
Attn: Mr. J. Bethke, Code 60C2	
P.O. Box 5152	
Warminster, PA 18974-0591	

**DISTRIBUTION LIST (Continued)**  
Report No. NAWCADWAR-92102-60

	No. of Copies
American Cyanamid Corporation .....	1
Attn: Mr. R. Kreiger	
Old Post Road	
Havre de Grace, MD 21078	
Bell Helicopter/Textron Inc. ....	1
Attn: Technical Library	
P.O. Box 482	
Fort Worth, TX 76101	
Commanding Officer .....	1
U.S. Army R&T Laboratory (ARRADCOM)	
Attn: R. Bonk	
Building 182	
Dover, NJ 07801	
National Aeronautics and Space Administration .....	1
(NASA Headquarters)	
Attn: Code RV-2	
600 Independence Avenue, SW	
Washington, DC 20546	
Administrator .....	1
National Aeronautics and Space Administration	
Attn: Airframes Branch, FS 120	
Washington, DC 20546	
Brigham Young University .....	1
Attn: Dr. William Pitt	
Chemical Engineering Department	
Provo, UT 64602	
Administrator .....	1
National Aeronautics and Space Administration	
George C. Marshall Space Flight Center	
Attn: Technical Library	
Huntsville, AL 35812	
Michigan Molecular Institute .....	1
Attn: Dr. Roger Morgan	
1910 W. St. Andrews Road	
Midland, MI 48640	
Commander .....	1
U.S. Naval Postgraduate School	
Attn: Technical Library	
Monterey, CA 93943	

**DISTRIBUTION LIST (Continued)**  
Report No. NAWCADWAR-92102-60

	No. of Copies
Lockhead Aeronautical Systems Company . . . . .	1
Attn: Technical Library	
P.O. Box 551	
Burbank, CA 91520	
Lockheed-Georgia Company . . . . .	1
Attn: Technical Library	
86 South Cobb Drive	
Marietta, GA 30063	
Boeing Military Airplane Company . . . . .	1
Attn: Technical Library	
P.O. Box 20746	
Wichita, KS 67277-7730	
General Dynamics/Convair Division . . . . .	1
Space Systems Division	
Attn: Technical Library	
P.O. Box 85990	
San Diego, CA 92138	
General Dynamics/Fort Worth Division . . . . .	1
Attn: Technical Library	
P.O. Box 748	
Fort Worth, TX 76101	
Boeing Helicopter Company . . . . .	1
Attn: Technical Library	
P.O. Box 16858	
Philadelphia, PA 19142	
Boeing Company . . . . .	1
Attn: Technical Library	
P.O. Box 3707	
Seattle, WA 98124-2207	
Administrator . . . . .	1
National Aeronautics and Space Administration	
Lewis Research Center	
Attn: Technical Library	
21000 Brookpark Road	
Cleveland, OH 44153	
Administrator . . . . .	1
Defense Technical Information Center	
Building #5, Cameron Station	
Alexandria, VA 22314	



**DISTRIBUTION LIST**  
Report No. NAWCADWAR-92102-60

	No. of Copies
Office of Naval Technology .....	1
Attn: W. King, ONT-212	
800 N. Quincy Street	
Arlington, VA 22217	
Rockwell International .....	1
North American Aircraft Division	
Attn: Technical Library	
P.O. Box 92098	
Los Angeles, CA 90009	
Sikorsky Aircraft .....	1
Attn: Technical Library	
North Main Street	
Stratford, CT 06601-1381	
McDonnell-Douglas Helicopter Company .....	1
Attn: Technical Library	
5000 E. McDowell Road	
Mesa, AZ 85205	
Northrup Aircraft Corporation .....	1
Attn: Technical Library	
One Northrup Avenue	
Hawthorne, CA 90250	
Northrup Aircraft Corporation .....	1
Attn: Anna Yen	
One Northrup Avenue	
Hawthorne, CA 90250	
Lockheed-Georgia Company .....	1
Attn: Technical Information	
Dept. 72-34, Zone 26	
Marietta, GA 30063	
McDonnell-Douglas Aircraft Company .....	1
Attn: Gail Hahn, M/S 0341200	
P.O. Box 516	
St. Louis, MO 63166	
Grumman Aerospace Corporation .....	1
Attn: Dr. T.M. Donnellan, M/S A01-26	
South Oyster Bay Road	
Bethpage, Long Island, NY 11714-3580	